

**SORPTION STUDIES OF CESIUM AND BARIUM
ON MAGNESITE USING RADIOTRACER AND
X-RAY PHOTOELECTRON SPECTROSCOPY**

**A THESIS
SUBMITTED TO THE DEPARTMENT OF CHEMISTRY
AND THE INSTITUTE OF ENGINEERING AND SCIENCES
OF BILKENT UNIVERSITY
IN PARTIAL FULFILLMENT OF THE REQUIREMENTS
FOR THE DEGREE OF
MASTER OF SCIENCE**

**By
TALAL SHAHWAN**

June 1997

90
547
.352
1997

SORPTION STUDIES OF CESIUM AND BARIUM
ON MAGNESITE USING RADIOTRACER AND
X-RAY PHOTOELECTRON SPECTROSCOPY

A THESIS
SUBMITTED TO THE DEPARTMENT OF CHEMISTRY
AND THE INSTITUTE OF ENGINEERING AND SCIENCES
OF BILKENT UNIVERSITY
IN PARTIAL FULFILLMENT OF THE REQUIREMENTS
FOR THE DEGREE OF
MASTER OF SCIENCE

By
TALAL SHAHWAN

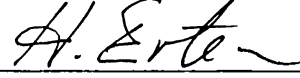
June 1997

Talal Shahwan

4D
547
.552
1997

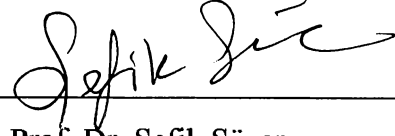
B037972

I certify that I have read this thesis and that in my opinion it is fully adequate, in scope and in quality, as a thesis of the degree of Master of Science



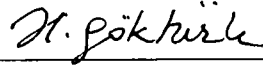
Prof. Dr. Hasan N. Erten (Principal Advisor)

I certify that I have read this thesis and that in my opinion it is fully adequate, in scope and in quality, as a thesis of the degree of Master of Science



Prof. Dr. Şefik Süzer

I certify that I have read this thesis and that in my opinion it is fully adequate, in scope and in quality, as a thesis of the degree of Master of Science



Prof. Dr. Hale Göktürk

Approved for the Institute of Engineering and Sciences



Prof. Dr. Mehmet Baray
Director of Institute of Engineering and Science

ABSTRACT

SORPTION STUDIES OF CESIUM AND BARIUM ON MAGNESITE USING RADIOTRACER AND X-RAY PHOTOELECTRON SPECTROSCOPY

TALAL SHAHWAN

M.S. in Chemistry

Supervisor: Prof. Dr. Hasan N. Erten

June 1997

As the consumption of the radioactive materials is continuously increasing, the problem of disposing the resulting wastes safely is becoming more challenging. One way through which these radioactive wastes could be isolated from the biological environment is by disposing them in deep geological formations. Clay minerals are proposed as backfill buffering materials that can delay the migration of the radionuclides and thus decrease the contamination of underground waters.

The extent of retardation of the radionuclide migration is dependent on factors like time of contact, pH and Eh of groundwater, concentration, temperature and grain

size of the mineral particles. Up to now, several studies were carried out to examine the effect of such parameters on the sorption behavior of different radionuclides on various kinds of minerals.

This study was conducted to investigate the effects of time, concentration and temperature on the sorption behavior of cesium and barium ions on magnesite. Cesium and barium have the radioactive isotopes ^{137}Cs ($t_{1/2} = 30.1$ y) and ^{140}Ba ($t_{1/2} = 12.8$ d) produced in high yields during the fission process which are important in radioactive waste considerations. Magnesite is a mineral composed mainly of magnesium carbonate together with minor amounts of quartz and has a single exchangeable cation, Mg^{2+} .

The radiotracer method and x-ray photoelectron spectroscopy, which is a powerful surface sensitive tool, were used in this study. The results obtained from both methods complemented each others and were in good agreement. Kinetic studies of the sorption process show that equilibrium was approached within one day of contact for both of cesium and barium ions.

The data of the sorption of both cations using different concentrations at various temperatures were most adequately described by the Freundlich type isotherms which correspond to multilayer adsorption on heterogeneous surfaces. The values of the Freundlich constants k and n imply that barium ions have slightly larger adsorption

affinity and adsorption intensity than cesium ions. The adsorption data at low concentrations were also observed to obey the Dubinin-Radushkevich type isotherms which describe monolayer adsorption on heterogeneous or homogeneous surfaces. The adsorption data were very poorly described by the Langmuir type isotherms.

Thermodynamic parameters such as enthalpy change, ΔH° , entropy change, ΔS° and free energy change of adsorption, ΔG° , were calculated from the sorption data of cesium and barium ions at different temperatures. The values obtained for ΔH° and ΔS° were -37 kJ/mol, -0.09 kJ/mol.K and -13 kJ/mol, -0.009 kJ/mol.K for cesium and barium ions respectively. The negative ΔH° values indicate the exothermic nature of adsorption which means that low temperatures are favored. The decrease in entropy upon adsorption implied by the negative ΔS° values is indicative of the stability of adsorption for both cations.

The values of ΔG° at different temperatures were all negative indicating the spontaneity of the adsorption process for both cesium and barium ions. The magnitudes of ΔG° were seen to be within the 8-16 kJ/mol range which is the energy range of ion-exchange type processes.

Keywords: Sorption, Cesium, Barium, Magnesite, Batch Operation, Radiotracer Method, X-ray Photoelectron Spectroscopy, Distribution Ratio, Atomic Concentration Ratio, Isotherm Models, Enthalpy of Sorption, Entropy of Sorption, Gibbs Free Energy.

ÖZET

SEZYUM VE BARYUM İYONLARININ MAGNEZİT MİNERALİ ÜZERİNE TUTULMASININ RADYOKİMYASAL YÖNTEMLER VE X-IŞINI FOTOELEKTRON SPEKTROSKOPİSİ İLE İNCELENMESİ

TALAL SHAHWAN

Kimya Bölümü Yüksek Lisans

Tez Yöneticisi : Prof. Dr. Hasan N. Erten

Haziran 1997

Radyoaktif maddelerin artan üretim ve kullanımı sonucunda oluşan radyoaktif atıklar gün geçtikçe büyüyen bir sorun olarak ortaya çıkmaktadır. Bu atıkların derin jeolojik oluşumlara depolanması için planlar yapılmaktadır. Oluşumlarda bulunan kil mineralleri, radyoaktif izotopların dağılımını sorpsiyon yoluyla azaltmaktadır. Bunun sonucunda, bu izotopların yeraltı suların ulaşmaları ve meydana getirebilecekleri radyoaktif kirlenme önemli ölçüde önlenmektedir.

Radyoaktif maddelerin mineraller üzerine tutulma davranışları çeşitli faktörlerce etkilenmektedir. Bunların arasında temas süresi, yeraltısularının pH'ı ve Eh'i, iyon konsantrasyonu, ısı, ve mineral taneciklerin büyüklüğü sayılabilir. Bu faktörlerin sorpsiyon davranışları üzerinde olan etkilerini daha önceden birçok araştırmalarca incelenmiştir.

Bu çalışmada temas süresi, konsantrasyon ve ısı, sezyum ve baryumun iyonlarının magnezit üzerine sorpsiyonunu nasıl etkelediği araştırılmıştır. ^{137}Cs ($t_{1/2} = 30.1$ y) ve ^{140}Ba ($t_{1/2} = 12.8$ d) izotopları nükleer fizyon neticesinde yüksek verimle meydana gelen ve radyoaktif atıklar bakımından önemli olan radyoizotoplardır. Magnezit büyük ölçüde magnezyum karbonat az miktarda da kuartz içeren ve değişebilen tek iyonu olan bir mineraldir.

Bu çalışmalarda radyokimyasal yöntemle beraber güçlü bir yüzeysel teknik olan x-ışını fotoelektron spektroskopisi (XPS) de kullanılmıştır. Her iki yöntemden elde edilen sonuçların birbirlerinin tamamlayıcı ve birbirlerine uyum içinde olduğu gözlenmiştir.

Sezyum ve baryumun sorpsiyon kinetiği çalışmaları dengeye bir gün kadar bir sürede ulaşıldığı gösterilmiştir. Elde edilen sorpsiyon verilerine değişik izoterm

modelleri uygulanmıştır. Sorpsiyon verilerin Freundlich izoterm modeline en iyi uyduğu görülmüştür. Küçük konsantrasyonlarda verilerin ayrıca Dubinin-Radushkevich izoterm modeline de uyduğu gözlenmiştir. Verilerin Langmuir izoterm modeline uymadığı görülmüştür.

Değişik sıcaklıklarda elde edilen deneysel verileri kullanarak sorpsiyonda entalpi değişimi, ΔH° , entropi değişimi, ΔS° ve Gibbs serbest enerjisi değişimi, ΔG° , hesaplanmıştır.

Sezyum ve baryum iyonlarının ΔH° ile ΔS° değerleri -37 kJ/mol , -0.09 kJ/mol.K ve -13 kJ/mol , -0.009 kJ/mol.K olarak bulunmuştur. Her iki katyon için entalpi değişiminin eksi değerlerde olması sorpsiyon olayının ekzotermik olduğunu ve düşük sıcaklıklarda daha fazla katyon tutulduğunu göstermektedir. Diğer yandan, entropi değişiminin de eksi değerlerde olması sorpsiyonun her iki katyon için kararlı olduğunu göstermektedir.

Değişik sıcaklıklarda sezyum ve baryum için yapılan ΔG° hesaplamalarında negatif değerler elde edilmiştir. Bunlar ise, sorpsiyonun kendiliğinden oluştuğunu göstermektedir. Hesaplanan ΔG° değerlerinin tümü, $8-16 \text{ kJ/mol}$ değerleri arasında bulunmaktadır. Bu düzeydeki enerjiler, sorpsiyonun daha çok iyon değişimi yoluyla meydana geldiğini göstermektedir.

Anahtar Kelimeler: Sorpsiyon, Sezyum, Baryum, Magnezit, Ba Teknięi, Radyokimya, X-Iřını Elektron Spektroskopisi, Daęılım Oranı, Atom Konsantrasyonu Oranı, Izoterm Modelleri, Tutulma Entalpisi, Tutulma Entropisi, Gibbs Serbest Enerjisi.

ACKNOWLEDGEMENT

I would like to express my deep gratitudes towards my supervisor Prof. Dr. Hasan N. Erten for his cooperation and guidance throughout the course of this study.

I wish also to thank Prof. Dr. Şefik Süzer for his help and guidance in developing this thesis.

I debt thanks also to the department technicians, department secretary and to my friends for their help and encouragement.

I would like to express my endless thanks to my family and my wife for their unceased sacrifices and support throughout the course of my study.

TABLE OF CONTENTS

1. INTRODUCTION	1
1.1- Radioactive Waste Disposal	1
1.2- Groundwater and Radionuclide Migration	3
1.3- The Sorption Process	5
1.4- Cation Exchange Capacity	8
1.5- The Batch Technique	10
1.6- The Radiotracer Method	11
1.7- X-ray Photoelectron Spectroscopy	12
1.8- The Present Study	14
1.8.1- Cations and Their Radioactive Isotopes	14
1.8.2- Magnesite	15
2. MATHEMATICAL TREATMENT	20
2.1- The Distribution Ratio	20
2.2- The Atomic Ratio	22
2.3- Adsorption Isotherm Models	23
2.3.1- Langmuir Isotherm Model	24

2.3.2- Freundlich Isotherm Model.....	25
2.3.3- Dubinin-Radushkevich Isotherm Model.....	26
2.4- Thermodynamic Relationships.....	28
3. EXPERIMENTAL	30
3.1- Analysis of Bilkent Groundwater.....	30
3.2- Experiments Using the Radiotracer Method.....	31
3.2.1- Pretreatment of Magnesite Samples.....	31
3.2.2- Isotopic Tracers.....	31
3.2.3-Kinetic Studies.....	32
3.2.4- Studies of the Sorption Isotherms at Different Temperatures.....	32
3.3- Studies Using XPS.....	33
3.3.1-Kinetic Studies.....	34
3.3.2- Loading Experiments.....	34
3.3.3- Experiments at Different Temperatures.....	34
4. RESULTS AND DISCUSSIONS	36
4.1- Kinetic Studies.....	36
4.2-- Concentration and Temperature Dependence of Sorption.....	43
4.2.1- Loading Curves.....	43
4.2.2- Freundlich Isotherms.....	47
4.2.3- Dubinin-Radushkevich Isotherms.....	55

4.2.4- Langmuir Isotherms.....	58
4.3- Thermodynamic Parameters.....	60
4.4- Conclusions	72
REFERENCES.....	74

LIST OF FIGURES

1.1 (a) Structure of the Calcite Group, (b) Hexagonal Unit Cell, (c) Structure of Refractory Magnesia, $MgCO_3$	19
4.1 Variation of R_d Values as a Function of Time for Sorption of Cesium and Barium on Magnesite	40
4.2 Variation of Atomic Concentration Ratio as a Function of Time for Sorption of Cesium on Magnesite	41
4.3 Variation of Atomic Concentration Ratio as a Function of Time for Sorption of Barium on Magnesite	42
4.4 Variation of R_d as a Function of Cation Loading for the Sorption of Cesium on Magnesite	45
4.5 Variation of R_d as a Function of Cation Loading for the Sorption of Barium on Magnesite	46
4.6 Freundlich Isotherm Plots for the Sorption of Cesium on Magnesite at Various Temperatures	48

4.7 Freundlich Isotherm Plots for the Sorption of Barium on Magnesite at Various Temperatures	49
4.8 Photoelectron Spectra of Magnesite Before Sorption and Cs and Ba 3d Regions After Sorption of Cs ⁺ and Ba ²⁺ Ions on Magnesite	53
4.9 Variation of Atomic Concentration Ratio as a Function of Initial Concentration for for Sorption of Cesium and Barium on Magnesite	54
4.10 Dubinin-Radushkevich Isotherm Plots for Sorption of Cesium on Magnesite at Various Temperatures	56
4.11 Dubinin-Radushkevich Isotherm Plots for Sorption of Barium on Magnesite at Various Temperatures	57
4.12 Variation of R_d as a Function of Temperature for the Sorption of Cesium on Magnesite	65
4.13 Variation of R_d as a Function of Temperature for the Sorption of Barium on Magnesite	66
4.14 Variation of Atomic Concentration Ratio as a Function of Temperature for Sorption of Cesium and Barium on Magnesite	71

LIST OF TABLES

1.1	Natural Mechanisms Governing Migration of Radionuclides in Permeable Media	7
1.2	Cation Exchange Capacities for a Number of Minerals	8
1.3	Composition of Typical Natural and Sea-water Magnesite	18
3.1	Ionic Concentrations of Na^+ , K^+ , Ca^{2+} , Mg^{2+} in Bilkent Tapwater	30
3.2	Initial Cation Concentrations of Cesium and Barium Ions used in Studying the Effect of Concentration and Temperature on Sorption	33
4.1	The Average R_d Values Obtained as a Function of Time for Sorption of Cesium on Magnesite	37
4.2	The Average R_d Values Obtained as a Function of Time for Sorption of Barium on Magnesite	38
4.3	Variation of Atomic Concentration Ratios as a Function of Time for Sorption of Cesium and Barium on Magnesite	39
4.4	The Average R_d Values Obtained as a Function of Concentration and Temperature for Sorption of Cesium on Magnesite	44

4.5	The Average R_d Values Obtained as a Function of Concentration and Temperature for Sorption of Barium on Magnesite	44
4.6	Parameters of Freundlich Isotherm Fits to the Data for the Sorption of Cesium and Barium on Magnesite at Various Temperatures	50
4.7	Variation of Atomic Concentration Ratios as a Function of Initial Concentration for Sorption of Cesium and Barium on Magnesite	52
4.8	Cation Adsorption Capacity (C_m) of Magnesite Obtained from D-R Isotherm Model Using the Sorption Data of Cesium and Barium Ions at Low Concentrations	58
4.9	The Linear Correlation Coefficients for Langmuir Least Square Fits to the Sorption Data of Cesium and Barium on Magnesite	59
4.10	Values of the Enthalpy Change, ΔH° , and Entropy Change, ΔS° , Obtained from the Sorption Data of Cesium on Magnesite	62
4.11	Values of the Enthalpy Change, ΔH° , and Entropy Change, ΔS° , Obtained from the Sorption Data of Barium on Magnesite	63
4.12	Values of the Gibbs Free Energy Change of Adsorption, ΔG° , Obtained from the Sorption Data of Cesium and Barium on Magnesite	69
4.13	Variation of Atomic Concentration Ratios as a Function of Temperature for Sorption of Cesium and Barium on Magnesite	70

1. INTRODUCTION

1.1- Radioactive Waste Disposal

Safe disposal of the radioactive materials that are no longer useful to man is a big theme in many countries nowadays. The overall objective of radioactive waste disposal is to dispose the wastes in a manner which ensures that there is no unacceptable detriment to man and to the biological environment, as a whole at present and in the future. Waste confinement by the disposal system should remain effective until the radionuclides have decayed to acceptable levels, and are no longer forming a potential hazard to the human environment.

With a sufficient number of natural and man-made barriers, the release of radioactive materials can be limited or delayed, its transport retarded or its concentration sufficiently diluted to assure that impact on man will remain within acceptable levels.

According to the International Atomic Energy Agency, IAEA, five major options are valid for underground disposal of radioactive wastes [1]:

- 1- Disposal in shallow ground
- 2- Disposal in deep geological formations
- 3- Disposal in rock cavities
- 4- Disposal by liquid injection
- 5- Disposal by hydraulic fracturing

In general safe disposal of radioactive wastes is achieved by [2]:

1- Confinement of the waste in one or more natural or man-made barriers and thus its adequate isolation from the human environment, in particular from ground water.

2- Retardation of radionuclide migration if the waste is, or will be, in contact with ground water or subject to other migration mechanisms.

3- Disposal of the waste at a depth or location where future natural or man made disruptive events are extremely unlikely.

Appropriately conditioned wastes may be disposed of in an underground repository. Conditioning aims at immobilizing the radionuclides and packaging the waste in order to make it safer for handling, storage, transport and disposal. An underground repository consists of both natural geological environment and man made facilities. The geological environment of the repository includes the strata in which the wastes are emplaced, the surrounding strata and the natural materials of the land surface. The man made facilities include the excavated cavities, engineered features within the cavities, backfill and sealing materials, and facilities at or near the surface which are integral with the function of the underground repository (e.g engineered barriers to control erosion or waste movement, facilities for handling wastes etc.)

The function of the underground repository is to provide primary barriers for controlling possible radionuclide release from the emplaced waste to man so as to keep them at acceptable levels.

1.2- Groundwater and Radionuclide Migration

One way through which radionuclides could be transported to the biosphere is by groundwater flowing through a network of fractures in the surrounding rocks. The extent of release of radionuclides to the biosphere is minimized if the travel

times of water are sufficiently long in comparison with the half-lives of the radionuclides [3].

The migration process of the radionuclides by groundwater is affected much by various parameters . Among these parameters are; the pH, the redox potential, Eh, the total salinity of water and the concentration of potential complexing agents. pH determines the degree of hydrolysis and the ion-exchange. Eh determines the valence state for multivalent waste elements.

The pH of groundwater is influenced mainly by the presence of carbonates in the system. In the absence of air, Eh is largely determined by the presence of minerals containing natural metal redox systems [4].

A large amount of laboratory and field work is being carried out internationally to study the extent of radionuclide migration. Part of this work includes the determination of sorption, or distribution coefficients for fission products and actinides from a wide range of groundwater compositions on various geological materials. Sorption studies are being carried out on unaltered and altered rock, on unconsolidated mineral infillings from water bearing fractures and on the clay buffer and backfill materials [5].

1.3- The Sorption Process

Table 1 gives the different natural mechanisms governing migration of radionuclides in permeable media [6]. Sorption is one of the mechanisms that govern the migration of radionuclides in groundwater . It can affect radionuclide concentration and as a result retard or delay their migration into the biosphere. The sorption or desorption of radionuclides by soil fractions is affected by parameters like their concentration in groundwater, the contact time, temperature, pH, the grain size of soil particles, formation of colloids and others.

The terms sorption and adsorption are often used to describe the process by which radionuclides are removed from solution by a solid phase. Solutes which undergo sorption are commonly termed sorbates, and the solid phase as, the sorbing phase or sorbent.

Sorption or adsorption process is usually interpreted as a reversible ion exchange or surface sorption reaction that can be described by a sorption isotherm.

In general, the sorption process may be classified as [7]:

1- Physical Adsorption:

Non-specific attractive forces between the trace elements and the solid surfaces are responsible for physical adsorption. This kind of adsorption is generally

rapid, pH independent, reversible and relatively independent on temperature and concentration.

2- Electrostatic Adsorption:

Sorption occurs as a result of coulombic attractive forces between electrically charged surfaces and ions in solution. Ion exchange is an example of such kind of adsorption. This process is rapid, largely reversible, strongly dependent on the ionic strength and composition of the solution and to a certain extent temperature dependent.

3- Chemical Adsorption (Chemisorption):

Specific chemical forces involving chemical bonding between the dissolved component and the solid surface are responsible for this type of adsorption. Chemisorption is slow, partially irreversible, highly dependent on composition of the sorbent and concentration of the solute and often strongly temperature dependent.

Table 1.1: Natural Mechanisms Governing Migration of Radiouclides in Permeable Media.

Mechanism	Relevant Effect
Flow	Movement of a nuclide at the velocity of water
Diffusion	Movement of a nuclide within the fluid under a concentration gradient
Dispersion	Distribution of nuclides due to their velocity variations in porous media
Sorption	Reversible interaction between mobile and immobile phases. It includes ion exchange, ion adsorption and filtration. It leads to a retardation of the nuclide relative to the velocity of water
Immobilization	Irreversible interaction between mobile and immobile phases. It includes, for example, precipitation and co-precipitation.
Radioactive Decay	Process of natural radiochemical evaluation which determines the final species of radionuclides and their concentrations at the groundwater discharge zones

1.4- Cation Exchange Capacity

The process in which cations from natural waters are sorbed by mineral particles with the concurrent release of an equivalent amount of cations is termed as cation exchange process. The cation exchange capacity, CEC, of a component is the summation of the exchangeable cations. It is reported as milliequivalents of cation per 100 g of mineral. Different methods are proposed for the measurement of CEC of various minerals [8, 9, 10]. One of the most widely used methods is to measure the uptake of ammonium ions from 1M ammonium acetate solution at pH 7. Table 1.2 gives CEC values for a number of materials [11].

Table 1.2: Cation Exchange Capacities for a Number of Minerals

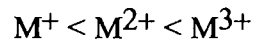
Material	Magnesite	Kaolinite	Illite	Chlorite	Humic Acids
CEC(meq/100g)	3-7	3-15	10-40	20-50	170-590

Values for CEC are pH dependent and vary as a function of the ion accompanying the exchange sites. There are several factors that will affect the exchange capacities;

- 1- Quality of clay and silt fractions. The silt fractions generally have an appreciable exchange capacity.
- 2- The kind of clay mineral present. As an example, a small quantity of illite can give a greater exchange capacity than a larger amount of kaolinite.
- 3- The amount of organic matter present. Organic matter increases the exchange capacity irrespectively of the clay mineral present.
- 4- Cation exchange capacity figures for the clay fractions are only a slight indication of the clay minerals present when mixtures of clay minerals occur. Hence the CEC figure should not be used as the only indication of the presence of certain clay minerals. The data should be supplemented with the x-ray diffraction analysis.

The affinity of a certain cation, M^+ , for an exchange site is affected by several factors, such as [12]:

- 1- Concentration in solution: As $[M^+]$ increases, there is an increase in the fractional surface coverage.
- 2- Oxidation state: An increase in the oxidation state of an element favours its accumulation at the surface, the order of affinity being:



3- Charge density of the hydrated cation: the greater the charge density, the greater is the affinity for an exchange site.

1.5- The Batch Technique

The batch technique is widely used in sorption studies which aims at investigating the effect of different parameters on the sorption behaviour of radionuclides.

In a batch operation, the adsorbent is contacted with the liquid phase in a container, for a period of time. The adsorbent is separated from the liquid by centrifugation, filtration or settling. The time required to approach equilibrium condition depends on the concentration of the solute, the amount of solid, the particle size of adsorbent and the degree of shaking.

For batch operations, the adsorbent is usually applied in powdered form to increase the surface area and reduce the diffusional resistance inside the pores.

Agitation of the suspension improves contact of particles with liquid and decreases the mass transfer resistance at the surface [13].

The important drawback of batch operation is believed to result from the continuous creation of fresh fracture surfaces as a result of shaking. This leads to increase in the surface areas in contact with the radionuclide solution and hence, increases the distribution ratio [14].

1.6- The Radiotracer Method

The radiotracer method is widely used in studies of the sorption characteristics of radioactive wastes on various minerals. The experimental procedure consists of spiking a solution containing the stable isotope of a certain element in the ionic form with the radionuclide of that element, then contacting the solution with the geological mineral. The radionuclide concentration in an aliquot of the solution is monitored periodically during the sorption process. The decrease in the radionuclide concentration in solution is attributed to sorption by the mineral. The radioactive isotope added to a solution serves as a tracer because it behaves as the other inactive isotopes of the same element originally present in the same chemical form.

The radiotracer method was applied in this study, to examine the sorption behavior of cesium and barium on magnesite. The two elements possess the radioactive isotopes ^{137}Cs ($t_{1/2} = 30.17$ years) and ^{140}Ba ($t_{1/2} = 12.79$ day) which are produced in high yields during fission and are important from radioactive waste management view point.

Previously, a number of studies to examine the sorption properties of cesium and barium on different clay and soil fractions from various regions of Turkey, were carried out in the laboratories at Bilkent and at the Middle East Technical Universities using the radiotracer method [15 - 19].

1.7- X-ray Photoelectron Spectroscopy

X-ray photoelectron spectroscopy (XPS), is one of the most widely used surface sensitive technique. It comprises a group of techniques in which photoelectrons emitted from a sample, which is irradiated by electromagnetic radiation of a suitable wavelength, are separated on the basis of their kinetic energies and detected by a photomultiplier device which is then recorded in the form of electron yield against the electron energy. In XPS, the irradiating source is an x-ray beam and the photoelectrons are emitted from the core and valence levels of the constituent atoms of the sample.

Although originally conceived as an analytical technique, XPS can also give informations on the 'chemical environment' of constituent atoms. The information content of the XPS specrum may be considered in two parts; Elemental composition and chemical speciation. XPS is basically a form of atomic spectroscopy and, as such, it has a clear and well-defined analytical role based on the positions and sizes of peaks within the spectrum. However, the exact energy levels of the core and valence electrons respond to their electronic environment and additional structural or chemical information, may be obtained from binding energy shifts and spectral fine structure [20].

Application of XPS to sorption studies has shown an increase in the last decade. A number of studies in which XPS was used for obtaining qualitative and quantitative analytical informations and/or chemical and structural informations are available in literature [21 - 27]. XPS technique is really suitable for the study of sorption reactions for a number of reasons. First and foremost is that it is inherently surface sensitive. It is particularly versatile because it can detect any element of geochemical interest except hydrogen, it can be used to estimate surface coverage of sorbed species or thickness of their precipitate films, and it can provide important informations on the chemical state of the substrate surface before reaction, and both the substrate and sorbed species after reaction [28].

1.8- The Present Study

The sorption characteristics of a trace element are affected by a number of chemical and physical parameters, such as, the radionuclide concentration in solution, pH and ionic strength of the solution, the surface properties and surface to volume ratio of the solid phase, time of contact and temperature of the medium.

In the present study, the batch technique was used in examining the effect of time, concentration and temperature on the sorption behaviour of Cs^+ and Ba^{2+} ions on magnesite by the radiotracer method and x-ray photoelectron spectroscopy, XPS.

1.8.1- Cations and Their Radioactive Isotopes

Barium is an alkaline earth element, its radioactive isotope ^{140}Ba ($t_{1/2} = 12.79$ day) is a fission product with a high yield. This radionuclide is a serious radiocontaminant during the first 100 days when fission products are discharged into the environment. Furthermore, Ba being a homolog of Ra is a suitable cation for the radiochemical study of Ra, which have several radioisotopes that are important in waste considerations. ^{133}Ba was chosen as a suitable tracer in our studies because of its long half life (10.7 years) and well observable γ -ray of 361 keV energy.

^{137}Cs ($t_{1/2} = 30.17$ years), a product of the nuclear age, is produced by the nuclear fission reaction in high yield. No natural sources of ^{137}Cs exist, thus its presence in the environment is due to either nuclear weapons testing or disposal of the radioactive wastes of nuclear reactors or nuclear accidents like Chernobyl in 1986. ^{137}Cs is a principal radiocontaminant due to its long half life. It emits a strong γ -ray (662 keV) making its measurement in environmental samples relatively easy and accurate.

1.8.2- Magnesite

Magnesite is a member of the isomorphous group of minerals that includes calcite and dolomite. The structure of magnesite is similar to that of calcite but with a slightly smaller cell due to the smaller size of magnesium ion as shown in Figure 1.1. Magnesite commonly occurs in veins and irregular masses derived from the alteration of Mg-rich metamorphic and igneous rocks through the action of water containing carbonic acid. Such magnesites are compact, crystalline and often contain opaline silica. Beds of crystalline cleavable magnesite are (i) of metamorphic origin associated with talc schists, chlorite schists, and mica schists, and (ii) of sedimentary origin formed as a primary precipitate or as a replacement of limestones by Mg-containing solutions, dolomite being formed as an intermediate product [29].

Magnesite resembles dolomite in being only slightly soluble in cold dilute HCl, but it dissolves with effervescence in warm acids. It differs from dolomite and calcite in having higher refractive indices [30].

The mineral magnesite crystallizes in the hexagonal system and has rhombohedral cleavage. Individual crystals of magnesite are rare and the mineral is commonly massive. It occurs commercially as crystalline masses, which resembles marble or coarse-grained dolomite, and as a cryptocrystalline (amorphous) masses, which have a dense porcelainlike texture and conchoidal fracture. There is some variation in color but the mineral is generally white or grayish. The specific gravity is between 2.9 to 3.1 and hardness ranges from 3.5 to 4.5. Like calcite and dolomite, magnesite loses carbon dioxide on heating. Calcining at 1450-1750°C drives off all the carbon dioxide except about 0.5 percent yielding a dense, sintered, inert product called refractory magnesia [31]. The structure of this resulting product (MgO) is given in Fig. 1.1(c).

The major deposits of natural magnesite, often associated with limestone and dolomites, occur in Austria, -previous- Czechoslovakia, Greece, Yugoslavia, Russia, Canada, the United States, Brazil and North East China.

Sea-water magnesite has largely replaced natural magnesite in countries where minor deposits of magnesite exist. Sea-water magnesite, used in industry, is

obtained by chemical reactions involving sea-water and calcium hydroxide and differs slightly in composition from natural magnesite. Compositions of typical natural and sea-water magnesite samples are given in Table 1.3 [32].

Magnesite, contains a single cation, Mg^{2+} , that can be exchanged with other cations. It is possible that $MgCO_3$ loses Mg^{2+} and accepts instead other divalent or monovalent cations. In addition, if any isomorphous substitution of a Si atom by another atom (e.g Al) in any array of SiO_2 tetrahedra structure occurs, a negatively charged framework will be established. This charge is localized, and relatively strong surface complexes with cations can be formed [33].

Table 1.3: Composition of Typical Natural and Sea-water Magnesite Samples

Oxide	Natural Magnesite	Sea-water Magnesite
	Weight (%)	Weight (%)
SiO ₂	1.50	0.8
Al ₂ O ₃	0.07	0.5
Fe ₂ O ₃	0.54	1.3
CaO	2.90	0.8
B ₂ O ₃	0.01	0.15
Cr ₂ O ₃	0.01	-
MgO	94.97	96.4

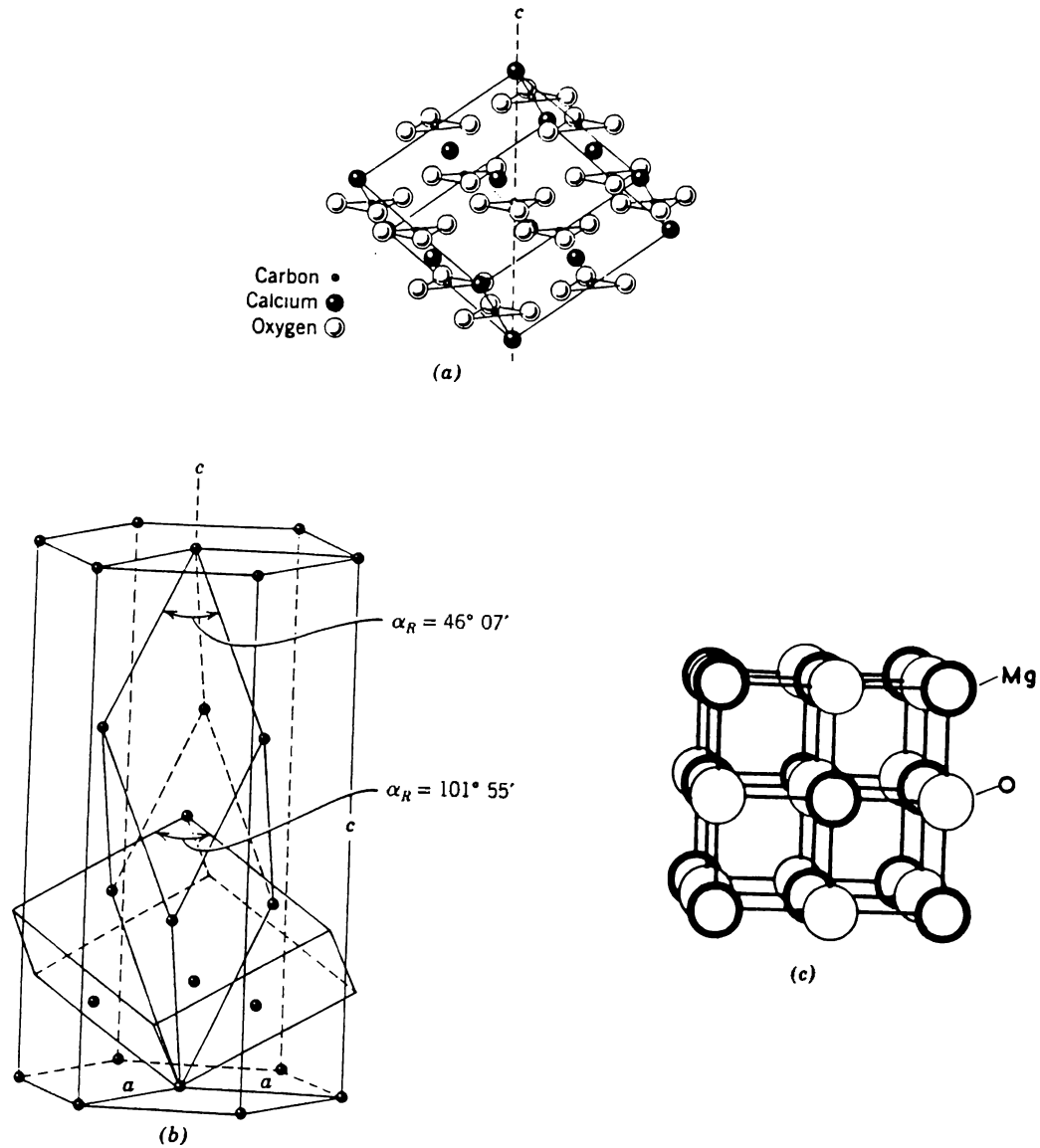


Fig. 1. 1: (a) Structure of calcite group (b) The relation of the steep, true unit cell to the cleavage rhombohedron, which is face-centered. A hexagonal cell is also shown (c) Structure of refractory Magnesia, MgO.

2. MATHEMATICAL TREATMENT

2.1- The Distribution Ratio

The distribution ratio, R_d , of a certain species represents its concentration at the solid phase to that in the liquid phase:

$$R_d = \frac{m_s/M}{m_l/V} \quad (2.1)$$

where m_s , m_l are the masses of the nuclide (meq) at the solid phase and in the solution respectively, M is the mass of the solid phase (g) and V is the volume of the solution (mL).

In sorption studies, R_d aids in quantifying the extent of retardation of a certain trace element by the solid phase from solution under certain conditions. In the experimental determination of R_d , the the behavior of a radioactive isotope is

monitored periodically by measuring its activity in the liquid phase. It is assumed that the physical and chemical properties of the stable isotope do not differ from that of the radioactive isotope for an element, and thus R_d can be used to describe the behavior of that element rather than the behavior of the radio-isotope alone.

The equation above relates to a reversible sorption. Yet often a portion of sorbed nuclide does not desorb, so there is a need to define distribution ratios for adsorption and desorption separately. The distribution ratio of adsorption, $R_{d,ad}$ for a component C is expressed as:

$$R_{d,ad} = \frac{[C]_{s, ad}}{[C]_{ad}} \quad (2.2)$$

Where $[C]_{s,ad}$ (meq/g) and $[C]_{ad}$ (meq/mL) are the concentrations of species C in the solid and liquid phases respectively. At the beginning of the sorption step, V (mL) of solution with initial concentration $[C]^\circ$ (meq/mL) is used, and at the end of sorption step $V+\Delta W_{pt}$ (mL) of solution with concentration $[C]_{ad}$ are present, hence the concentration of C in the solid phase after sorption can be expressed as :

$$[C]_{s, ad} = \frac{V[C]^\circ - (V + \Delta W_{pt})[C]_{ad}}{W_s} \quad (2.3)$$

In terms of activity, $[C]_{ad}$ can be written as :

$$[C]_{ad} = \frac{A_{1,ad}}{A^\circ} [C]^\circ \quad (2.4)$$

From (2.1), (2.2), (2.3) and (2.4), the following equation is obtained :

$$R_{d,ad} = \frac{VA^\circ - (V + \Delta W_{pt})A_{1,ad}}{A_{1,ad}W_s} \quad (2.5)$$

where :

A° =initial count rate of solution added for sorption (cps)/mL

$A_{1,ad}$ =count rate of solution after sorption (cps)/mL

W_s =weight of solid material (g)

ΔW_{pt} =amount of liquid remaining in the tube after pretreatment, before sorption (g,mL).

2.2- The Atomic Ratio

The elemental content of the samples analyzed by x-ray photoelectron spectroscopy, XPS, can be identified from the corresponding peaks in the spectrum. The fact that the intensities of these peaks (their areas) are proportional to the elemental concentrations of the atoms or ions within the sample forms the basis of

the quantification analysis. In this analysis, first it is necessary to choose an element whose content remains constant before and after sorption. Then the peak intensities of the other elements in the same sample are normalized with respect to the observed intensity of the chosen element. The atomic ratio can then be calculated from the observed intensities using the formula [34]:

$$[A]/[B] = (I_A/I_B) (\sigma_B/\sigma_A) (E_k(B)/E_k(A))^{3/2} \quad (2.6)$$

where $[A]/[B]$ is the atomic ratio of A and B, I is the observed intensity, σ is the tabulated cross section [35], and E_k is the kinetic energy ($h\nu - B.E$) of the electrons emerging from the analyzed sample.

2.3- Adsorption Isotherm Models

The equilibrium sorption data at a given temperature are usually represented by an adsorption isotherm, which is a relationship between the quantity sorbed per unit mass of solid and the concentration of the sorbate in solution. Many theoretical and empirical models have been developed to represent the various types of adsorption isotherms. Langmuir, Freundlich and Dubinin-Radushkevich are the most frequent isotherm models used for this purpose.

2.3.1- Langmuir Isotherm Model

A simple model of the solid surface is used to derive the equation of this isotherm. In this model, the solid is assumed to have a uniform surface at which there are no interaction between one sorbed molecule and another, the sorbed molecules are localized at specific sites and only a monolayer can be sorbed. The Langmuir isotherm is given as:

$$C_s = \frac{b \cdot C_m \cdot C}{1 + bC} \quad (2.7)$$

where:

C_s : Amount of solute sorbed per unit mass of solid (meq/g)

C_m : Maximum amount of solute sorbed by the solid (meq/g)

C : Equilibrium concentration of solute in solution (meq/mL)

b : A constant related to the energy of sorption

When the sorbate concentration becomes very low, the equation approaches linearity.

The equation above may be rearranged to lead to the linear form:

$$C_s = C_m - \frac{C_s}{bC} \quad (2.8)$$

By plotting C_s versus C_s/C , a straight line is obtained. The slope of that line gives $1/b$ and the intercept gives C_m . The distribution ratio, R_d , can be obtained by rearranging the above equation to give:

$$R_d = \frac{bC_m}{1+bC} \quad (2.9)$$

2.3.2- Freundlich Isotherm Model

Fruendlich isotherm is the most widely used non-linear model for describing the dependence of sorption on concentration. The general expression can be written as:

$$C_s = k C_1^n \quad (2.10)$$

where:

C_s : amount of solute sorbed per unit weight of solid (meq/g)

C_1 : equilibrium solute concentration (meq/mL)

k and n : constants

The expression above can be linearized to give:

$$\log C_s = \log k + n \log C_l \quad (2.11)$$

Plotting $\log C_s$ versus $\log C_l$ yields n as the slope and $\log k$ as the intercept.

Freundlich isotherm model allows for several kinds of adsorption sites on the solid, each kind having a different heat of adsorption. The Freundlich isotherm represents well the data at low and intermediate concentrations and is a good model for heterogeneous surfaces.

Equation (2.10) can be rearranged to give the distribution ratio, R_d :

$$R_d = k C_l^{n-1} \quad (2.12)$$

2.3.3- Dubinin-Radushkevich Isotherm Model

This isotherm resembles Langmuir isotherm in being applicable at low trace concentrations, but differs in not requiring homogeneous adsorption sites. The equation is given as:

$$C_s = C_m \exp(-K\epsilon^2) \quad (2.13)$$

where

ϵ : Polanyi potential, $RT\ln(1+1/C)$

C : solute equilibrium concentration in solution (meq/mL)

R : gas constant

T : absolute temperature (K)

K : constant

C_m : sorption capacity of adsorbent per unit weight (meq/g)

C_s : observed amount of solute sorbed per unit weight (meq/g)

The linear form of the equation above may be obtained by rearranging it to give:

$$\ln C_s = \ln C_m - K\epsilon^2 \quad (2.14)$$

If $\ln C_s$ is plotted against ϵ^2 , K and $\ln C_m$ will be obtained from the slope and the intercept, respectively. Equation (2.13) may be written in a form that gives R_d :

$$R_d = (1/C)C_m \exp(-K\epsilon^2) \quad (2.15)$$

2.4- Thermodynamic Relationships

Gibbs Free energy change (kJ/mol) is defined for a chemical process by the following equation:

$$\Delta G = \Delta G^{\circ} + RT \ln K \quad (2.16)$$

where R is the gas constant , T is the absolute temperature (K) and K is the equilibrium constant. If the distribution constant is used as an equilibrium constant, where ΔG becomes zero, then the following equation can be written:

$$\Delta G^{\circ} = -RT \ln R_d \quad (2.17)$$

In literature , another expression of ΔG° exists. This expression relates Gibbs free energy change to the enthalpy and entropy changes. The equation is given as:

$$\Delta G^{\circ} = \Delta H^{\circ} - T\Delta S^{\circ} \quad (2.18)$$

If equations (2.17) and (2.18) are equated and rearranges for $\ln R_d$, the following expression can be obtained :

$$\ln R_d = \frac{\Delta S^\circ}{R} - \frac{\Delta H^\circ}{RT} \quad (2.19)$$

where R is the gas constant (=8.314 J/mole.K)

Equation (2.19) approximates R_d as a fully equilibrium constant and assumes the enthalpy to be constant within the entire temperature range. This equation was used by many authors [36, 37, 38] in the determination of the enthalpy and entropy changes, and it was applied in our thermodynamic calculations for the same purpose. Plotting $\ln R_d$ vs $(1/T)$, the enthalpy change can be determined from the slope and the entropy change from the intercept. For the determination of Gibbs free energy of adsorption (ΔG°), equation (2.17) was used.

3. EXPERIMENTAL

3.1- Analysis of Bilkent Groundwater

Bilkent tapwater -as a substitute for groundwater- was used in the pretreatment of the mineral samples which were used later in the radiotracer studies. the concentrations of each of the primary cations Na^+ , K^+ , Ca^{2+} and Mg^{2+} in tapwater was determined by atomic absorption and atomic emission spectrometries in analytical chemistry laboratory at METU. Table 3.1 gives the concentrations of these cations.

Table 3.1: Concentrations of Na^+ , K^+ , Ca^{2+} and Mg^{2+} Ions in Our Laboratory Tapwater Used in Sorption Studies

Cation	Concentration (meq/mL)
Na^+	3.54×10^{-4}
K^+	1.21×10^{-4}
Ca^{2+}	2.67×10^{-4}
Mg^{2+}	4.38×10^{-4}
pH	6.85-7.20

3.2- Experiments Using the Radiotracer Method

3.2.1- Pretreatment of Magnesite Samples

The pretreatment step aimed to mimic the equilibrium situation of the magnesite samples with groundwater prior to sorption experiments. Tubes were first cleaned, dried at 60°C overnight, cooled and weighed. 30 mg of magnesite and 3 mL of our laboratory tapwater as substitute for groundwater were added into each tube that were then shaken for 4 days with a lateral shaker at 125 rpm. The shaker provided continuous shaking of the thermostate in which the tubes of samples were placed. Samples were then centrifuged at 6000 rpm for 30 minutes and the supernatant phases were discarded. Each tube was weighed again, and from the weight difference the amount of water left after pretreatment (ΔW_{pt}) was determined. The pretreated solid samples were later used in the sorption experiments carried out by the radiotracer method.

3.2.2- Isotopic Tracers

The tracers used in the sorption experiments carried out by the radiotracer method were ^{137}Cs with a specific activity of 5325 Bq/mL and ^{133}Ba with a specific activity of 1126 Bq/mL. Appropriate amounts of stable isotopes solutions were spiked with the corresponding radionuclides solutions used in the different

experiments. The count rates of the particular peaks for the two solutions were measured as 3901 cpm for 3 mL cesium solutions and 3957 cpm for 3 mL barium solutions.

3.2.3-Kinetic Studies

To each of the samples, 3 mL solutions (1×10^{-3} meq/mL of Cs^+ and 1×10^{-4} meq/mL of Ba^{2+}), prepared from CsCl and $\text{BaCl}_2 \cdot 2\text{H}_2\text{O}$ salts, with appropriate amounts of ^{137}Cs or ^{133}Ba radiotracers were added, separately. Sample tubes were shaken at room temperature for periods ranging from half an hour to eight days. Samples were then centrifuged and 2 mL portions of the liquid phases were counted using a Spectrum 88 instrument with a calibrated Ge detector connected to a multichannel analyzer.

3.2.4- Studies of the Sorption Isotherms at Different Temperatures

The effect of concentration and temperature on sorption was studied for each of the initial cation concentrations given in Table 3.2. Experiments were carried out at four different temperatures : 30, 40, 50 and 60°C. Three mL of the cation solution of interest containing an appropriate amount of radiotracer was added to each sample tube containing 30 mg of magnesite at the desired temperature. Temperature was maintained constant using a thermostated water bath.

The samples were shaken for one day, centrifuged and 2 mL portions of the liquid phase were counted.

Table 3.2: Initial Cation Concentrations of Cs⁺ and Ba²⁺ Used in Studying The Effect of Temperature on Sorption

Cation	Concentration (meq / mL)					
	1.00×10^{-1}	1.00×10^{-2}	1.00×10^{-3}	1.00×10^{-4}	1.00×10^{-5}	1.00×10^{-6}
Cs ⁺	1.00×10^{-1}	1.00×10^{-2}	1.00×10^{-3}	1.00×10^{-4}	1.00×10^{-5}	1.00×10^{-6}
Ba ²⁺	-	1.07×10^{-2}	2.15×10^{-3}	-	1.00×10^{-5}	1.00×10^{-6}

3.3- Studies Using XPS

The XPS technique was used in this study to carry out qualitative and quantitative analysis of the extent of exchange in the samples. Spectra of the samples were recorded using a KRATOS ES-300 spectrometer with Al K_α (hν=1486.3 eV) source. Samples were introduced as powders pressed on adhesive copper tapes, and the pressure in the analyzer chamber was kept below 10⁻⁸ torr during analysis. For calibration purposes C 1s line (B.E =285.0 eV) was used. This peak arised in the spectra as a result of residual or deposited hydrocarbons on the surface. Silicon content was assumed to be constant before and after the exchange, therefore Si 2p peak was used to normalize the intensity of the peaks belonging to other elements.

3.3.1-Kinetic Studies

Three mL portions of 0.1M Cs⁺ or Ba²⁺ solutions were added to 30 mg magnesite samples. Exchange was carried out at room temperature for periods starting from an hour up to several days. Mineral samples were then filtered and dried at 60°C for 24 hours. Then the XPS spectra were recorded. Cs and Ba 3d_{5/2} peak areas were used to calculate the atomic concentrations of each species in the samples.

3.3.2- Loading Experiments

To 30 mg magnesite samples 3 mL portions of solutions containing 1, 0.1, 0.01, 0.001M Cs⁺ or Ba²⁺ cations were added in each case. Exchange was carried at room temperature by shaking for one day. Samples were then filtered, dried and their XPS spectra were recorded.

3.3.3- Experiments at Different Temperatures

To study the temperature effect on sorption, experiments were done at 30, 40, 50, 60 and 70°C . Three mL 0.1M cation solutions were added to 30 mg magnesite samples both of which were previously brought to the desired

temperatures and samples were shaken for one day. The phases were then separated by filtration, dried and the XPS spectra were recorded.

4. RESULTS AND DISCUSSIONS

4.1- Kinetic Studies

The sorption kinetics of Cs^+ and Ba^{2+} ions on magnesite were studied by the radiotracer method and x-ray photoelectron spectroscopy, XPS, in order to determine the time required to approach the equilibrium state. This equilibrium time was later used as a fixed parameter in the studies carried out to examine the effect of other parameters on the sorption process. The results of the experiments carried out by the radiotracer method were expressed in terms of the distribution ratio, R_d . These results are given in Tables 4.1, 4.2 and plotted in Fig. 4.1 for Cs^+ and Ba^{2+} ions respectively.

The results show that equilibrium is approached within about a day of contact for both cases. In the Cs sorption case, the R_d values show an exponential increase in the first hours of contact, followed by a slight decrease leading to an equilibrium

Table 4.1: The Average R_d Values Obtained for the Sorption of Cs^+ on Magnesite as a Function of Time

Time of Contact	R_d (mL/g)
1 hour	21 ± 4
2 hours	31 ± 4
6 hours	38 ± 5
1 day	35 ± 5
2 days	43 ± 5
3 days	30 ± 4
5 days	32 ± 5
7 days	28 ± 5

plateau. In the Ba sorption case, however, the equilibrium plateau is not clear as such and the R_d values vibrate up and down before arriving to the equilibrium value. Such a behavior indicates that in the first hours of sorption, rapid accumulation of the sorbates on the sorption surface occur, followed by desorption of a small portion of the solutes and diffusion of the others toward the sorptive sites so that equilibrium is approached. Fig. 4.1 shows that this process is faster in Cs case than it is in the case of Ba.

Table 4.2: The Average R_d Values Obtained for the Sorption of Ba^{2+} ion on Magnesite as a Function of Time

Time of Contact	R_d (mL/g)
30 min.	105 ± 6
90 min.	102 ± 6
1 day	109 ± 6
2 day	79 ± 5
3 day	102 ± 5
4 day	73 ± 5
5 day	61 ± 5
6 day	72 ± 5
7 day	80 ± 5
8 day	83 ± 5

The experimental results of the XPS analysis were expressed in terms of the atomic concentration ratios calculated from the peak intensities which are then corrected for the kinetic energies and the cross sections as given in section 2.2.

The atomic ratios are given in Table 4.3 and plotted against time in Figs. 4.2 and 4.3 for the sorption of Cs^+ and Ba^{2+} ions respectively. The behavior of the

curves obtained by XPS method are similar to those obtained by the radiotracer method. Due to higher initial concentrations, somewhat shorter times of saturation were observed.

The rapid approach of equilibrium in both cases indicates that fast sorption steps are involved and suggests that ion-exchange at the surface might be the dominating sorption mechanism.

Table 4.3 : Atomic Concentration Ratios as a Function of Time for The Sorption of Cs^+ and Ba^{2+} on Magnesite Obtained by XPS Studies

Time of Contact (hour)	Atomic Ratio (Ba/Si)	Atomic Ratio (Cs/Si)
2	0.11	0.13
4	0.12	0.13
8	0.12	0.12
16	0.11	0.10
32	0.11	0.12
64	0.10	0.13

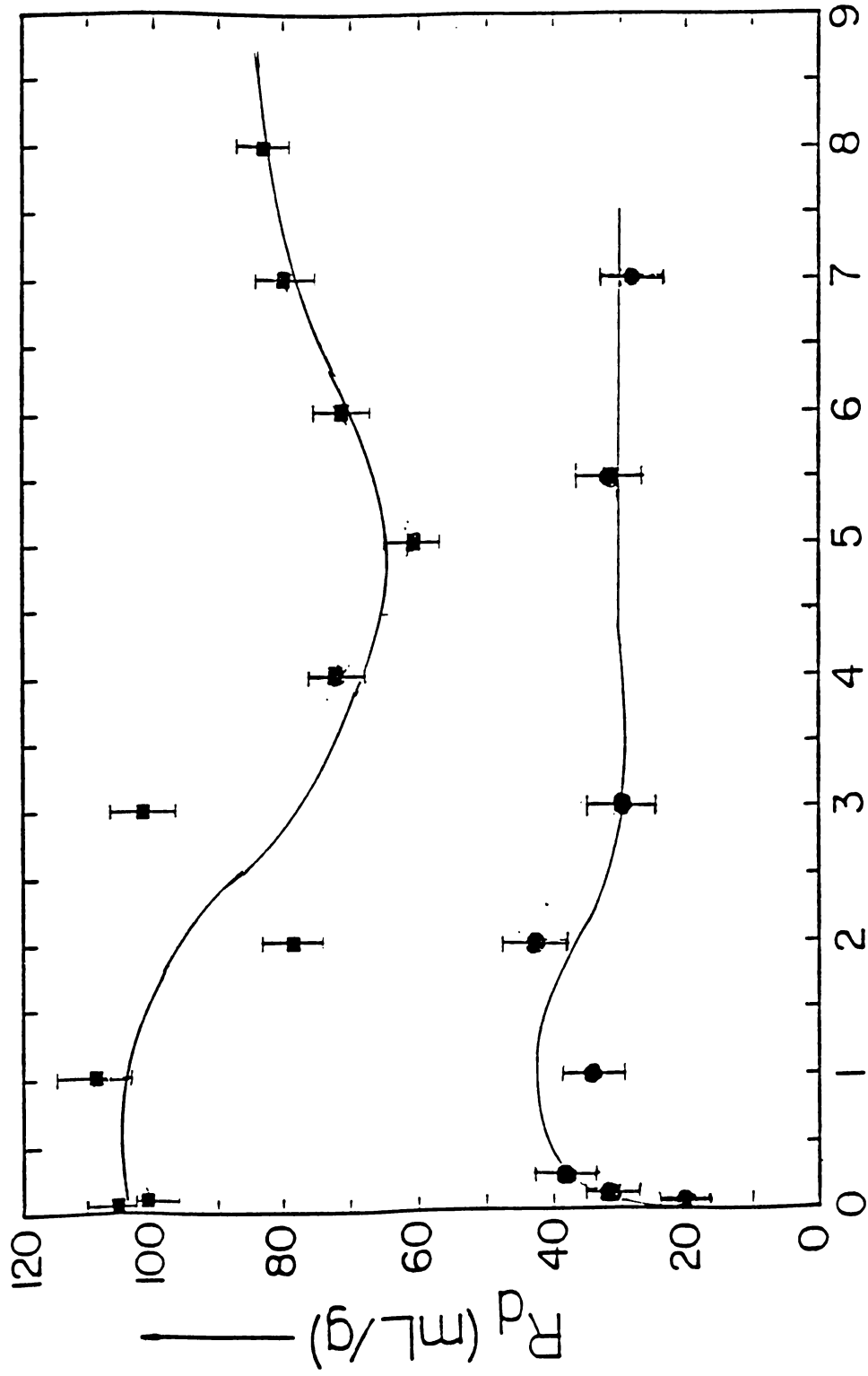


Fig. 4.1: Variation of R_d Values as a Function of Time for Sorption of Cesium and Barium on Magnesite. ■ : Barium ion ● : Cesium ion

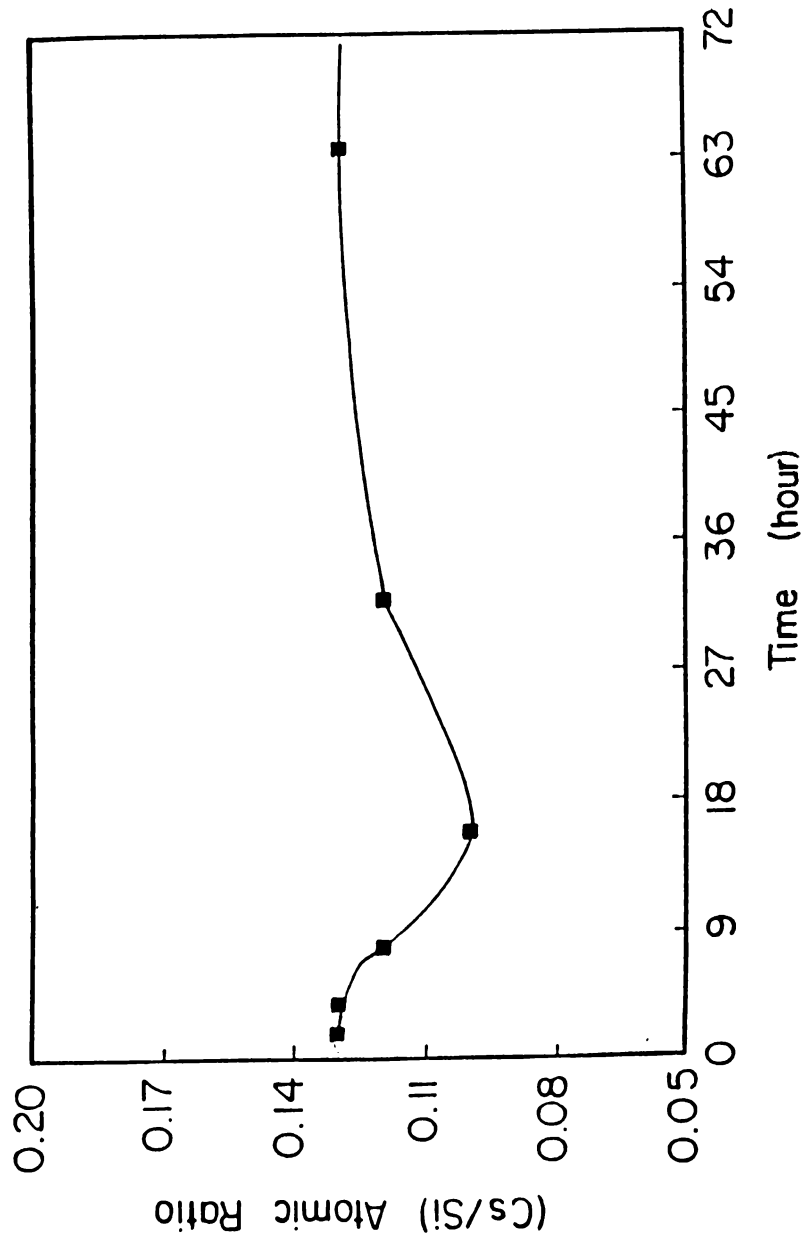


Fig. 4.2: Variation of Atomic Concentration Ratio as a Function of Time for Sorption of Cesium on Magnesite

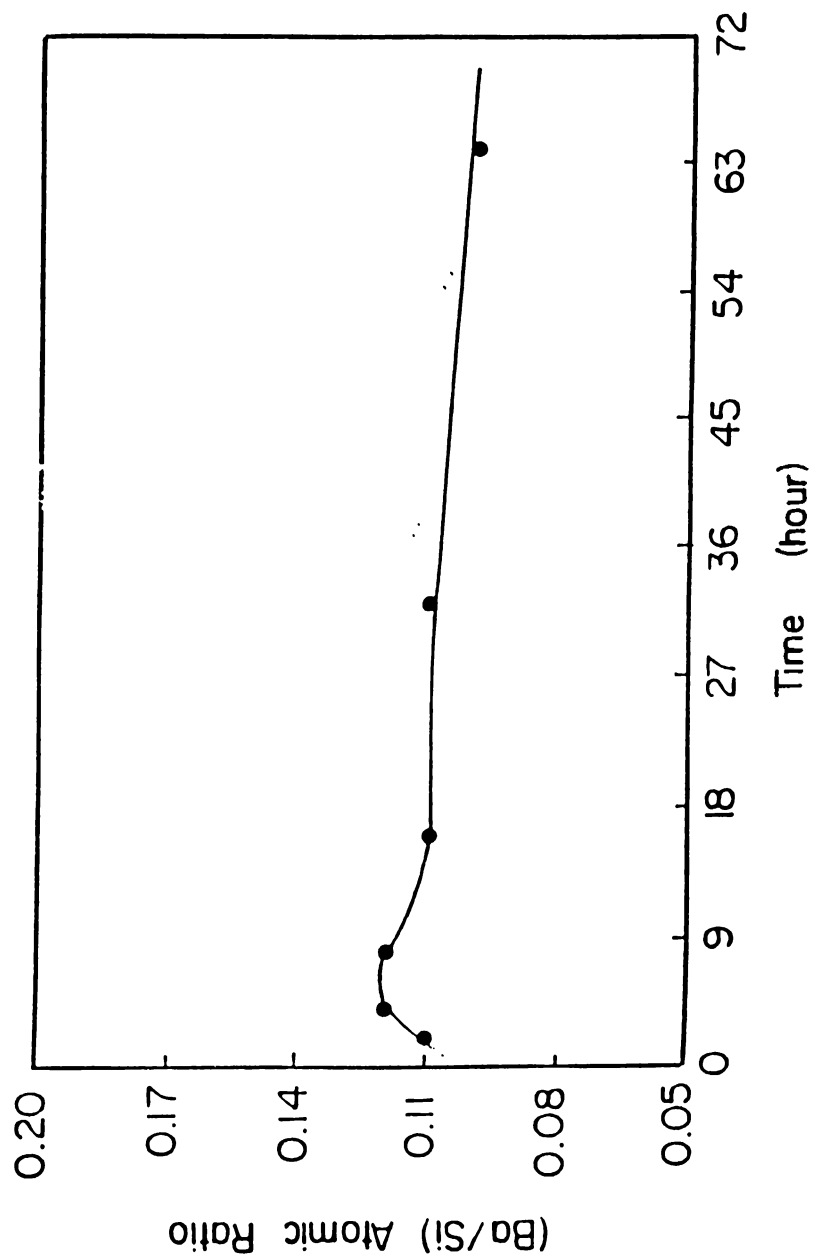


Fig. 4.3: Variation of Atomic Concentration Ratio as a Function of Time for Sorption of Barium on Magnesite

4.2-- Concentration and Temperature Dependence of Sorption

4.2.1- Loading Curves

The experimental values of the distribution ratio, R_d , obtained by the radiotracer method for the sorption of Cs^+ and Ba^{2+} ions at different initial concentrations and different temperatures are given in Tables 4.4 , 4.5 and plotted versus the cation loading in Figs. 4.4 and 4.5 respectively.

In Fig. 4.4, the loading curves show characteristic inverse S-shapes at all temperatures, suggesting that two different sorption sites on the solid matrix are present. This implies that cesium ion is sorbed via two mechanisms each corresponding to a different equilibrium constant. One equilibrium constant refers to a range of high R_d values, which most probably represent sorption at or near the surface of the solid matrix. The second equilibrium constant, however, corresponds to a range of lower R_d values that are supposed to refer to sorption on sites that lie inside the solid matrix. The R_d values obtained for the different cesium concentrations decrease as the sorption temperature increases. In the case of barium ion sorption, However, a single sorption site is suggested as shown in Fig. 4.5. Furthermore no significant temperature dependence of sorption was observed and R_d values show a constant plateau , then start to drop sharply upon increase in concentration.

Table 4.4 : The Experimental Values of R_d (mL/g) for the Sorption of Cs^+ on Magnesite at Different Initial Concentrations and Temperatures

Concentration (meq/mL)	R_d (mL/g)			
	303 K	313 K	323 K	333 K
1×10^{-1}	17 ± 6	15 ± 6	5 ± 4	5 ± 4
1×10^{-2}	24 ± 5	12 ± 7	8 ± 6	5 ± 4
1×10^{-3}	28 ± 7	28 ± 6	20 ± 6	9 ± 6
1×10^{-4}	102 ± 9	50 ± 7	23 ± 6	15 ± 6
1×10^{-5}	132 ± 10	89 ± 9	52 ± 7	65 ± 8
1×10^{-6}	225 ± 14	170 ± 12	127 ± 10	72 ± 8

Table 4.5: The Experimental Values of R_d (mL/g) for the Sorption of Ba^{2+} on Magnesite at Different Initial Concentrations and Temperatures

Concentration (meq/mL)	R_d (mL/g)			
	303 K	313 K	323 K	333 K
1.07×10^{-2}	18 ± 7	15 ± 6	19 ± 6	10 ± 6
2.15×10^{-3}	84 ± 9	51 ± 8	41 ± 7	41 ± 8
1.00×10^{-5}	83 ± 10	70 ± 10	76 ± 10	61 ± 9
1.00×10^{-6}	130 ± 13	118 ± 12	105 ± 12	93 ± 11

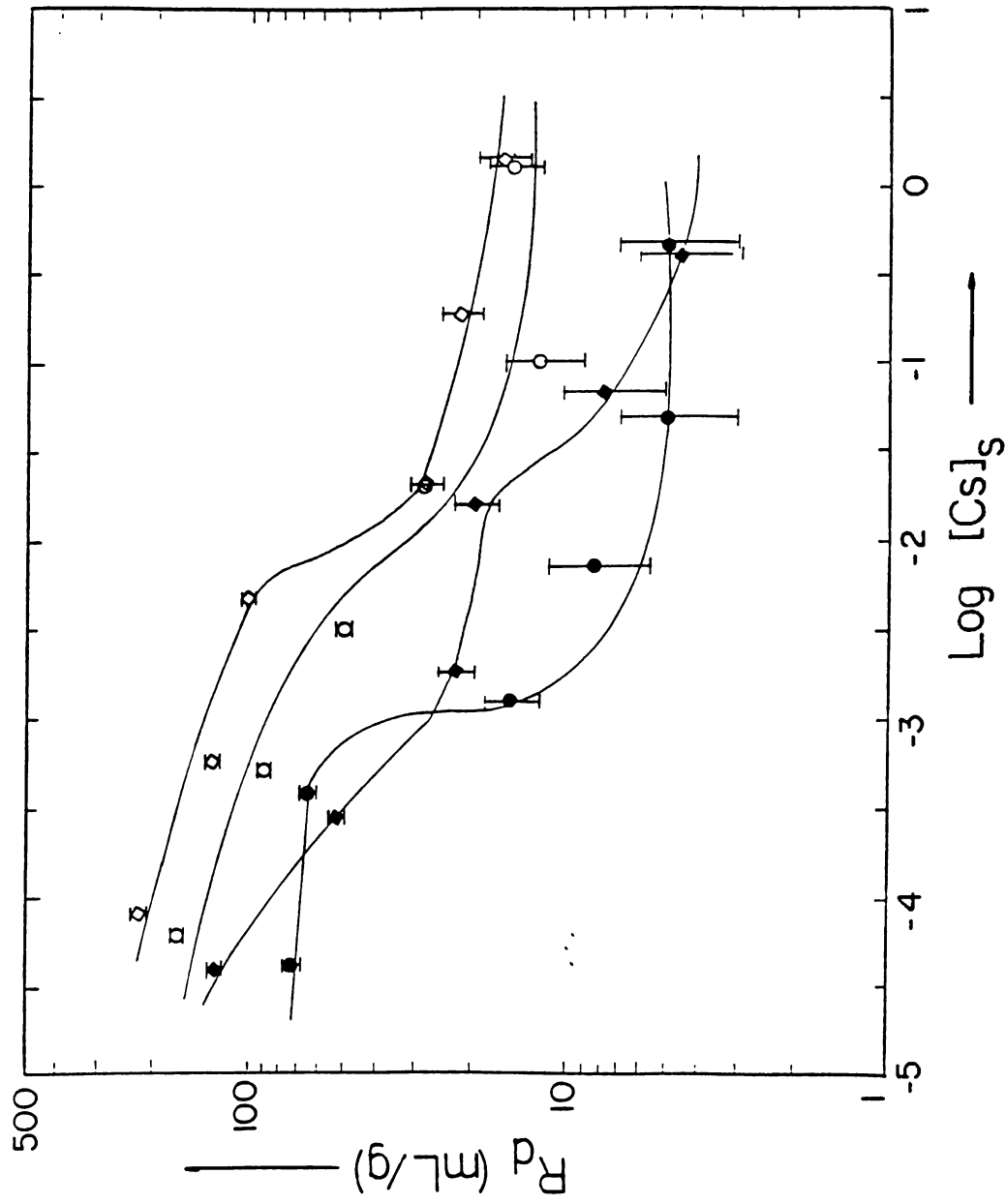


Fig. 4.4: Variation of R_d as a Function of Cation Loading for the Sorption of Cesium on Magnesite ◇ : T=30°C ○ : T=40°C ◆ : T=50°C ● : T=60°C

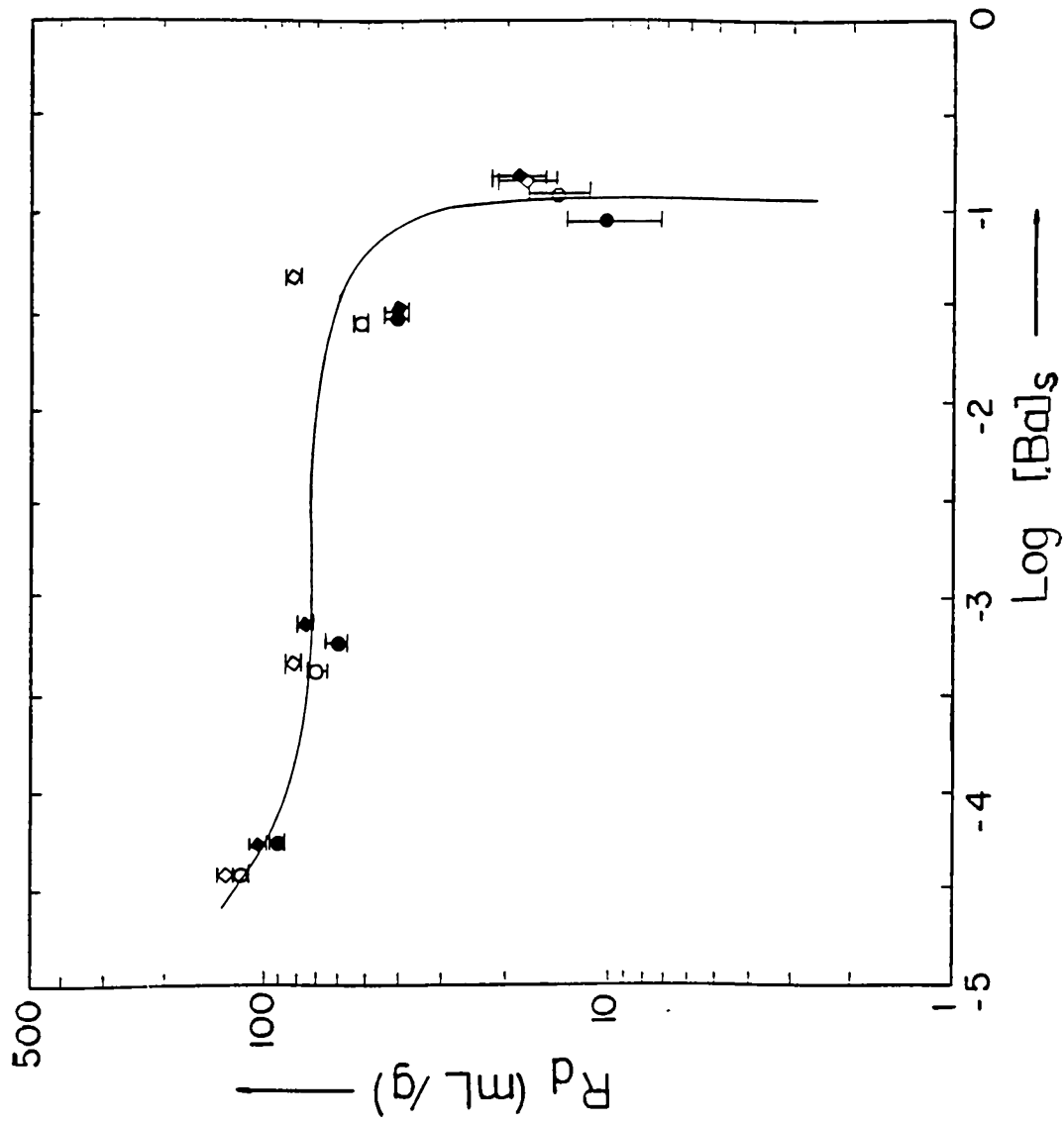


Fig. 4.5 : Variation of R_d as a Function of Cation Loading for the Sorption of Barium on Magnesite ◇ : T=30°C ○ : T=40°C ◆ : T=50°C ● : T=60°C

4.2.2- Freundlich Isotherms

Freundlich isotherm plots of the data obtained by the radiotracer method for the sorption of Cs^+ and Ba^{2+} ions on magnesite are shown in Figs. 4.6 and 4.7 respectively. As seen in the plots, Freundlich type isotherms provide an adequate description of the sorption behavior for all concentrations at different temperatures.

The results of the least square fits to the experimental data together with the linear correlation coefficient values (L.C.C) are given in Table 4.6. A higher value of the constant k indicates higher sorption affinity for ions in solution, whereas a higher value of n suggests higher sorption intensity. The numerical value of n (< 1.0), suggests that the surface of the sorbent is of heterogeneous nature [39]. At the limit when n equals unity, the sorption is said to be linear and the constant k becomes equivalent to the distribution ratio, R_d .

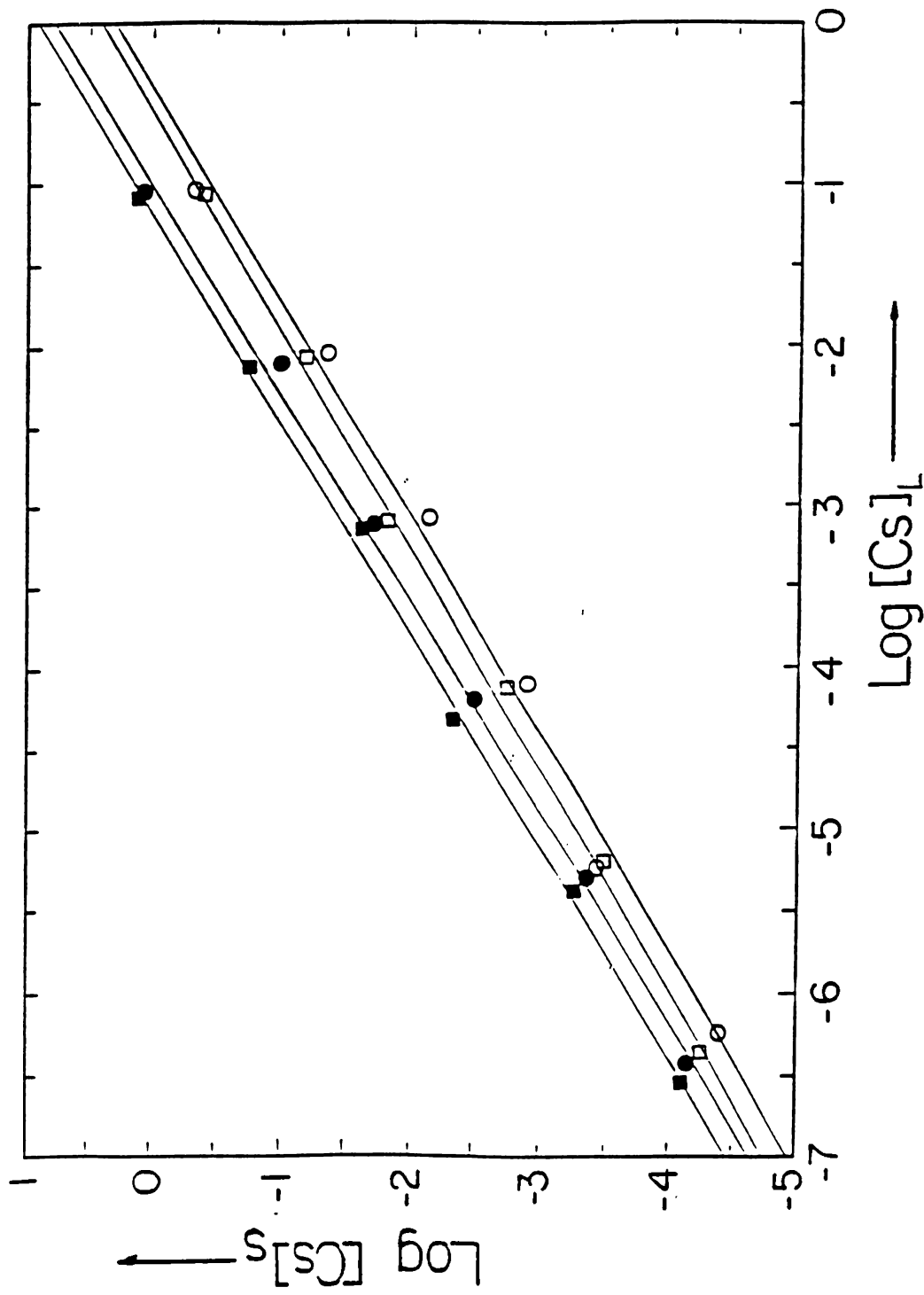


Fig. 4.6: Freundlich Isotherm Plots for the Sorption of Cesium on Magnesite at Various Temperatures ■ : T=30°C ● : T=40°C □ : T=50°C ○ : T=60°C

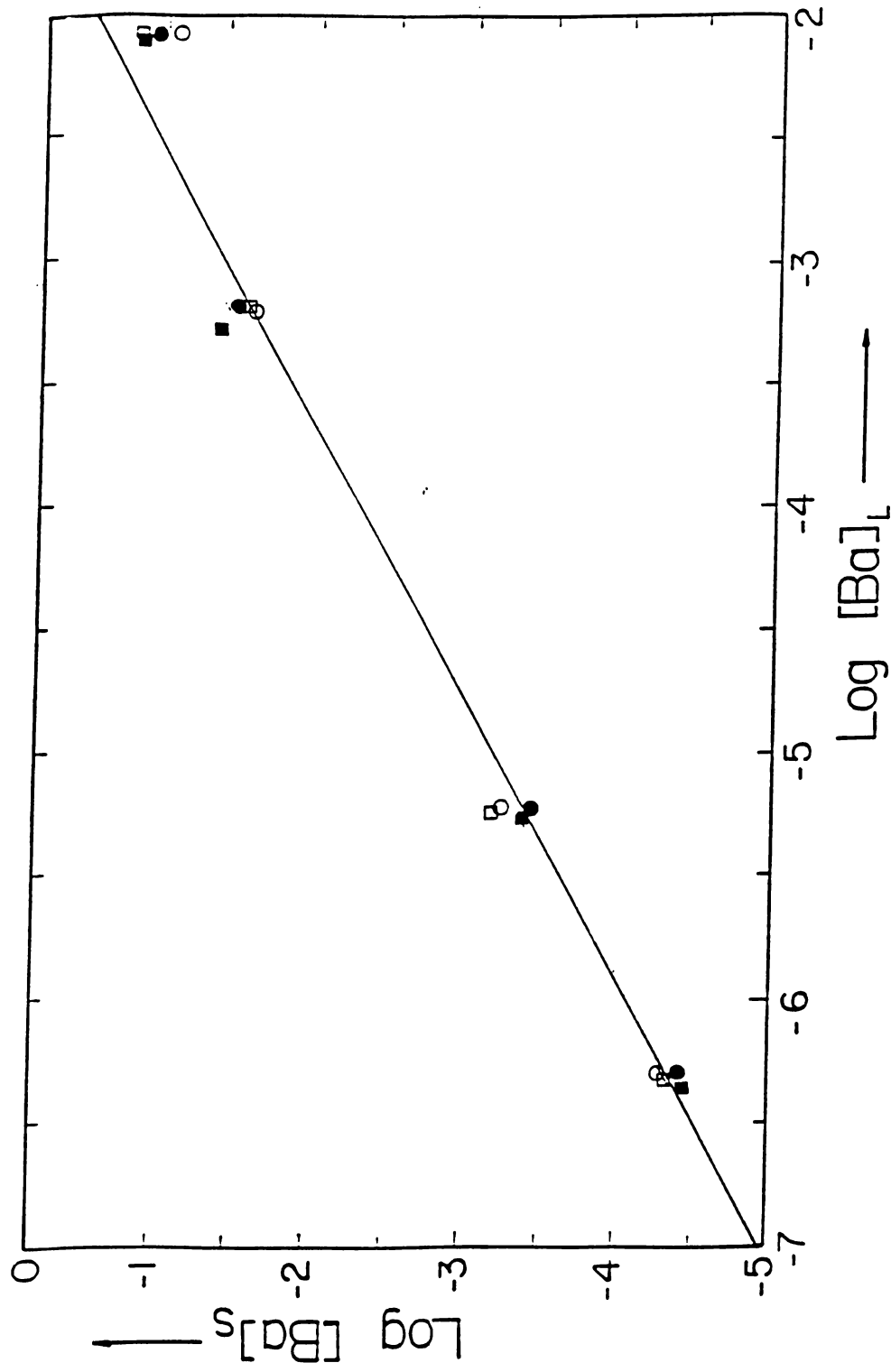


Fig. 4.7: Freundlich Isotherm Plots for the Sorption of Barium on Magnesite at

Various Temperatures ■ : T=30°C ● : T=40°C □ : T=50°C ○ : T=60°C

Table 4.6: Parameters for the Freundlich Type Isotherm Fits to the Data for the Sorption of Cs⁺ and Ba²⁺ Cations on Magnesite at Different Temperatures

T (K)	Cs ⁺			Ba ²⁺		
	k (meq/g)	n	L.C.C	k (meq/g)	n	L.C.C
303	7.9	0.77	0.998	16.2	0.87	0.991
313	4.0	0.75	0.999	10.4	0.85	0.995
323	2.4	0.74	0.999	9.1	0.81	0.997
333	1.8	0.74	0.995	5.9	0.80	0.992

It is interesting to observe that Ba²⁺ ion, has both higher affinity and higher sorption intensity than Cs⁺ ion. The sorption of both of Cs⁺ and Ba²⁺ ions at the same concentration is affected by two factors each acting in opposing directions. The first factor is the oxidation state and the second is the charge density of the hydrated ion. As was mentioned previously in section 1.3, an increase in the oxidation state favours the accumulation of the ion on the sorption surface leading to electrostatic stability, the thing that enhances the sorption of Ba²⁺ relative to that of Cs⁺. In contrast, the size of the hydrated barium ion is larger than that of cesium

ion which is likely to be sorbed as 'naked' cation owing to its low hydration energy [40], the thing that hinders the sorption of the former cation. The results obtained for n and k shows that the effect of the first factor exceeds that of the second, slightly in the case of Cs^+ and Ba^{2+} ions sorption on magnesite.

Furthermore, the n value of both species seems to be very slightly dependent on temperature. The k values of both Ba^{2+} and Cs^+ show however a drastic decrease with increasing temperature. The decrease for the latter is more pronounced, indicating that stability of Cs^+ sorption at higher temperatures is less than that of Ba^{2+} .

Fig. 4.8 shows an XPS spectrum of magnesite before sorption and the relevant regions of the spectrum after Cs^+ and Ba^{2+} sorption. Mg A refer to KLL Auger lines of Mg and one C 1s peak arises from CO_3^{2-} (the other one is due to the presence of some hydrocarbons). These peaks originate from the major component of magnesite, MgCO_3 . Si 2s and 2p peaks belong to quartz, the minor component of magnesite. The peaks of Cs and Ba refer to the photoemission of $3d_{3/2}$ and $3d_{5/2}$ electrons. The area of these peaks were used in expressing the amounts of Cs and Ba ions sorbed in terms of the cation concentration ratios.

The loading experimental results obtained by XPS are given in Table 4.7 in terms of the cation concentration ratios and plotted in Fig. 4.9. It is seen that the

amount of cations sorbed increases with increasing initial concentration. The increase in the cation concentrations is nonlinear for Cs and Ba ions sorption, the thing inline with what have been shown by Freundlich isotherms.

Table 4.7: The Atomic Concentration Ratios of Cesium and Barium Ions Obtained as a Function of Initial Concentration Using XPS technique

Concentration (M)	Atomic Ratio (Cs/Si)	Atomic Ratio (Ba/Si)
1.0	0.21	0.19
0.1	0.12	0.088
0.01	0.076	0.068
0.001	0.053	0.049

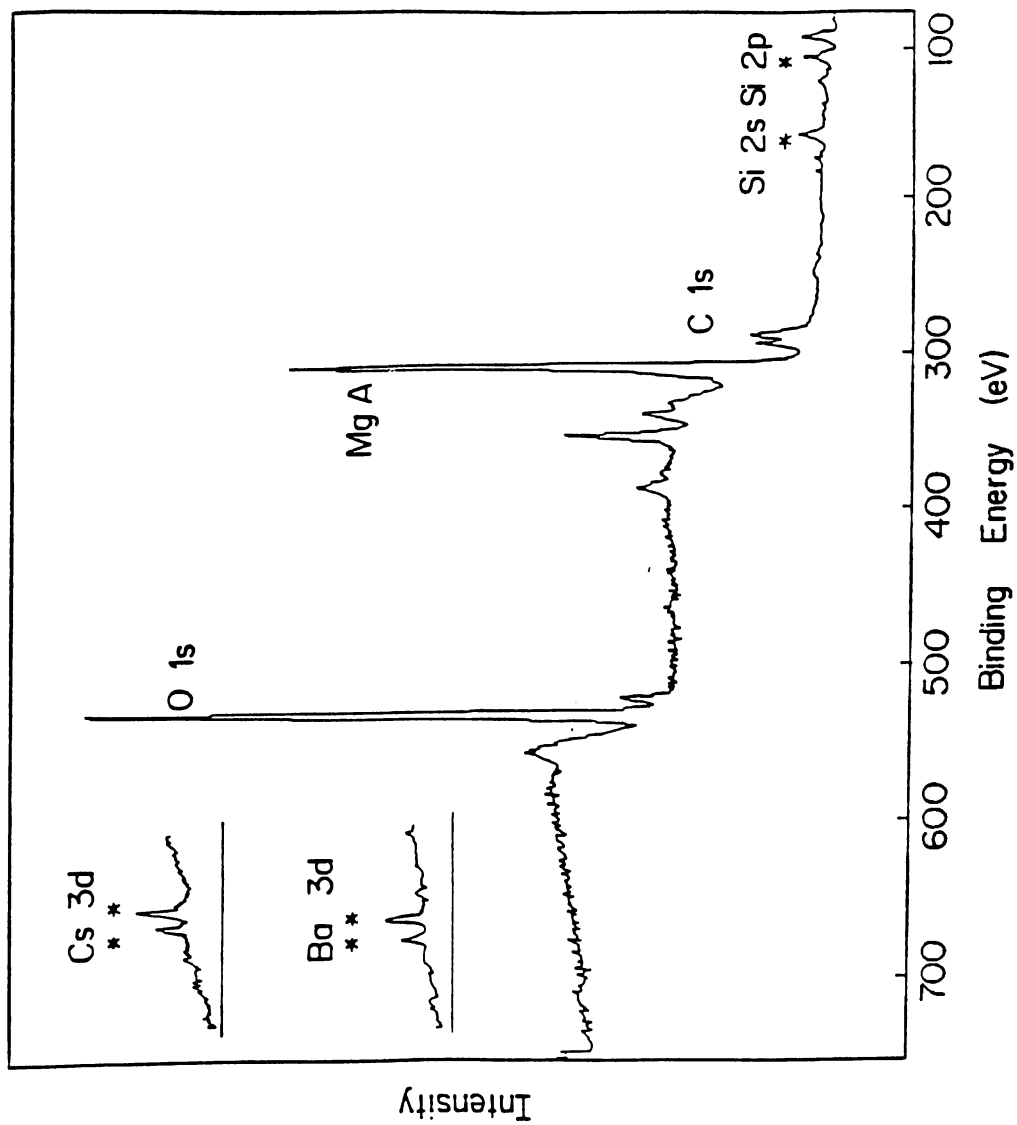


Fig. 4.8: Photoelectron Spectra of Magnesite Before Sorption and Cs and Ba 3d Regions After Sorption of Cs⁺ and Ba²⁺ Ions on Magnesite

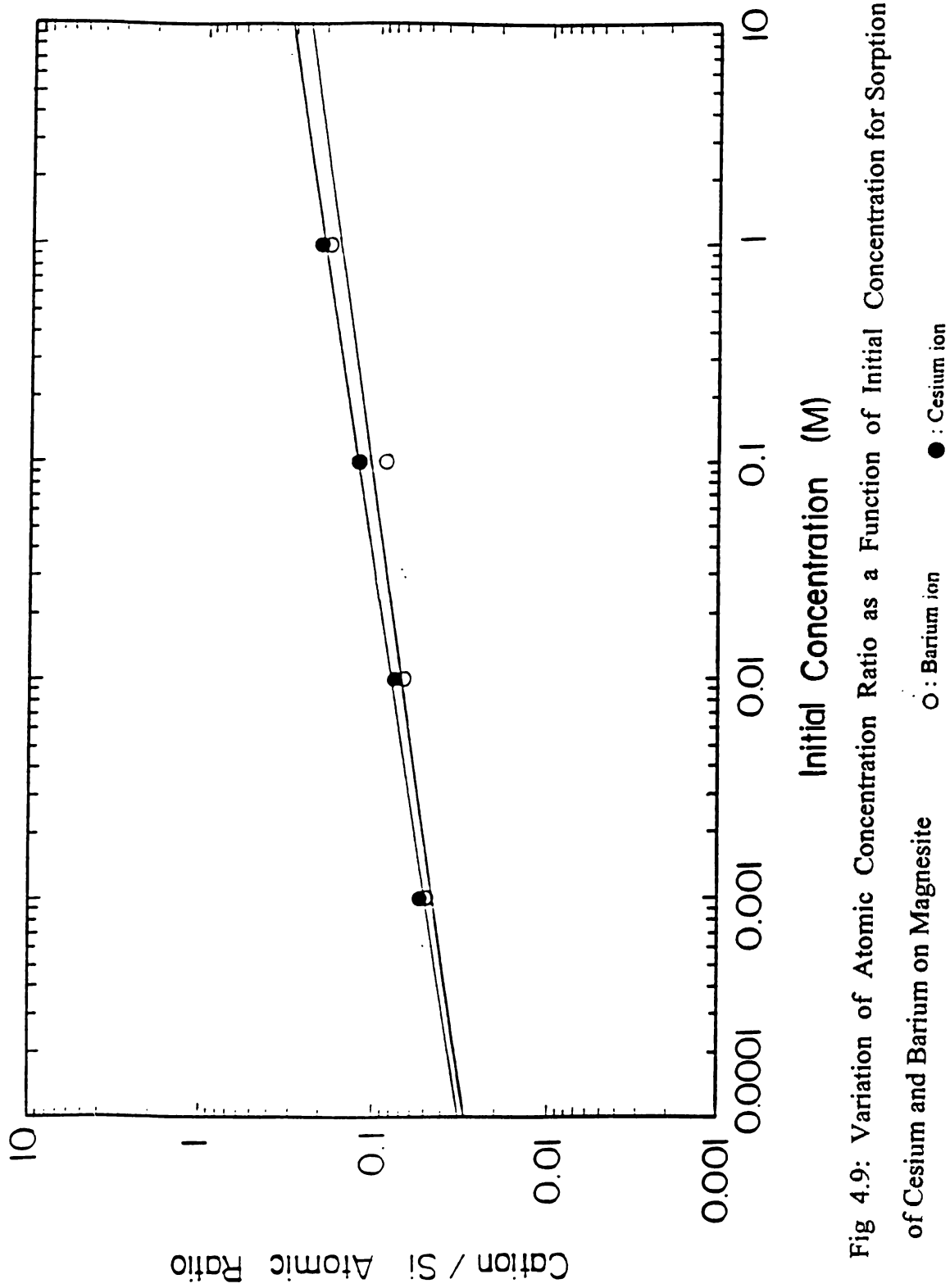


Fig 4.9: Variation of Atomic Concentration Ratio as a Function of Initial Concentration for Sorption of Cesium and Barium on Magnesite ○ : Barium ion ● : Cesium ion

4.2.3- Dubinin-Radushkevich Isotherms

The sorption data of Cs^+ and Ba^{2+} ions were fitted to Dubinin-Radushkevich (D-R) type isotherm as shown in Figs 4.10 and 4.11 respectively. As can be seen from the figures, this type of isotherms provide good description of the sorption data. At higher concentrations of Cs^+ ions, however, data deviate from linearity and as a result they were not included in the least square fits. This can be referred to the fact that D-R isotherm model was proposed for sorption of elements with low concentrations on homogeneous or heterogeneous surfaces.

When the lines used to fit the data are extrapolated toward the y-axis, the sorbent sorption capacity, which may be compared with the cation exchange capacity (CEC), can be estimated. Table 4.8 gives the sorption capacities of magnesite estimated from sorption of both of Cs^+ and Ba^{2+} ions. The sorption capacity values obtained from Cs^+ sorption data are comparable with the value given in literature for CEC of magnesite as 3-7 meq/100 g. These values are observed to decrease with increasing temperature which can be attributed to a decrease in the sorption of Cs^+ ions at higher temperatures. On the other hand, the values obtained from the Ba^{2+} sorption data are larger than the reported CEC value which might be an indication that there are mechanisms other than cation exchange involved in the Ba^{2+} sorption that give rise to the sorption capacity values.

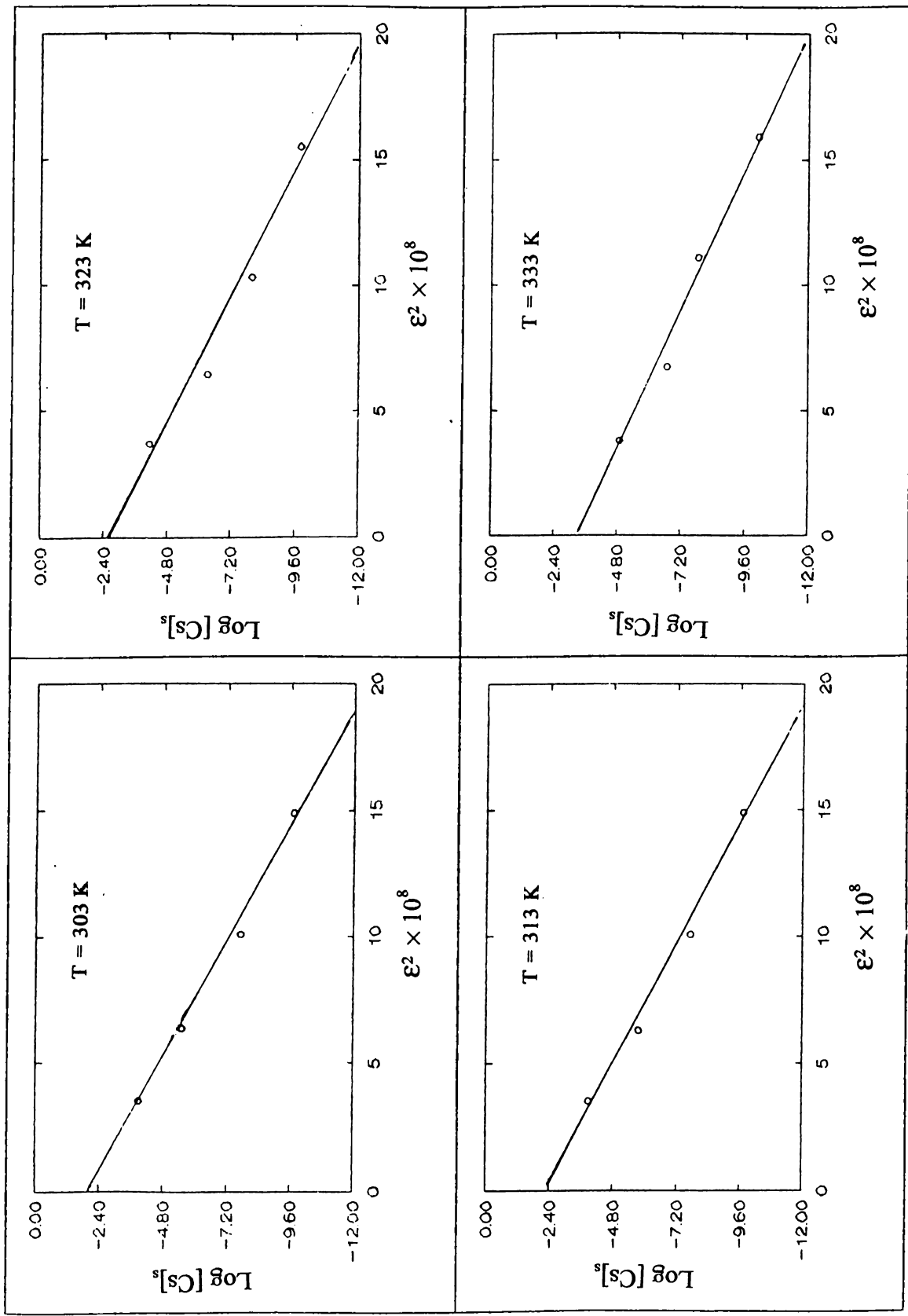


Fig. 4.10 : Dubinin-Radushkevich Isotherm Fits of the Adsorption Data of Cesium on Magnesite

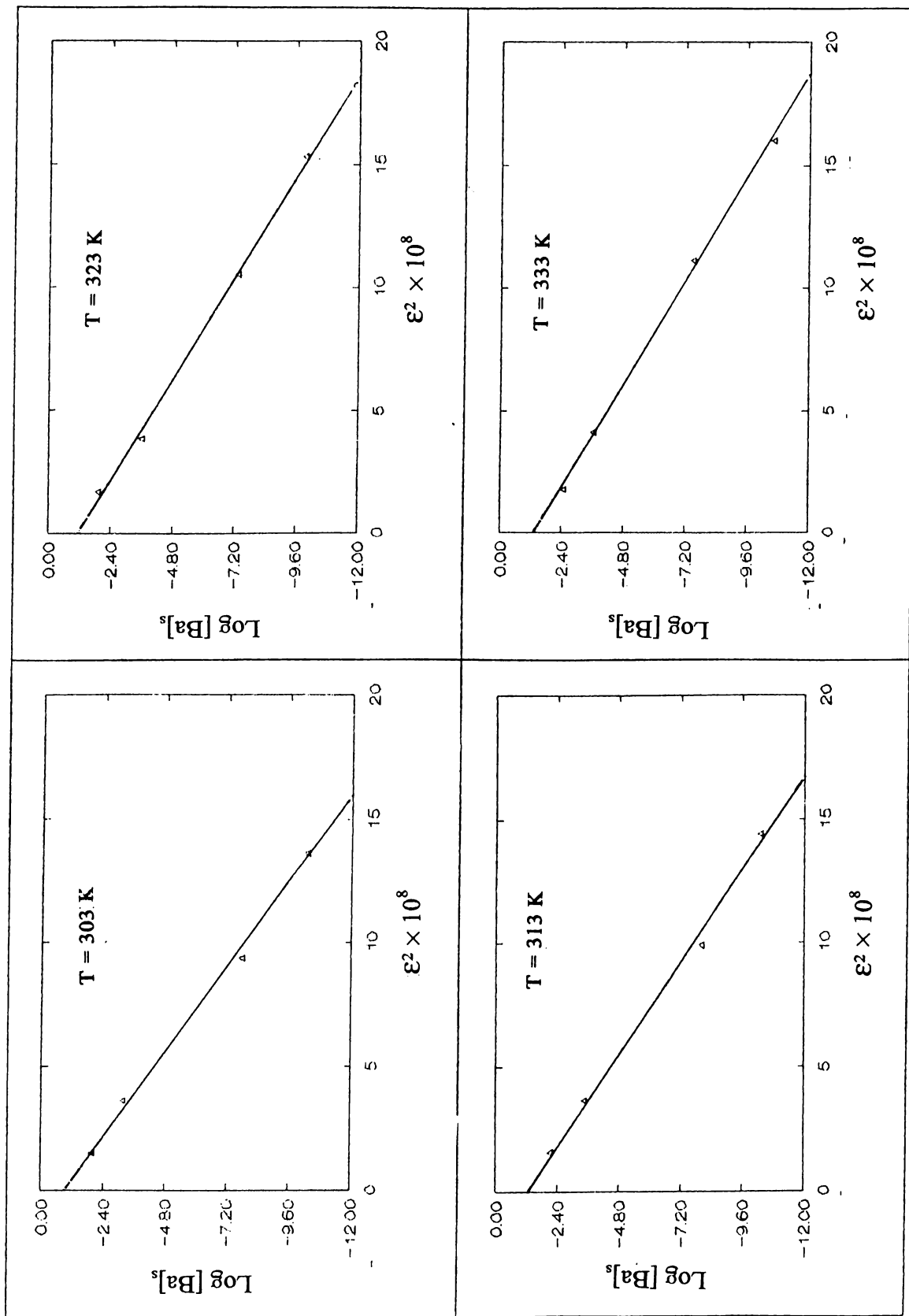


Fig. 4.11 : Dubinin-Radushkevich Isotherm Fits of the Adsorption Data of Barium on Magnesite

Table 4.8: Cation Sorption Capacity, C_m (meq/100g), of Magnesite Obtained From D-R Isotherm Model Using the Sorption Data of Cesium and Barium Ions at Low Concentrations

T (K)	Cs^+		Ba^{2+}	
	C_m	L.C.C	C_m	L.C.C
303	10.9	0.997	51.2	0.996
313	9.4	0.995	29.5	0.995
323	5.4	0.983	23.2	0.999
333	2.9	0.992	24.7	0.999

4.2.4- Langmuir Isotherms

Langmuir isotherm model, proposed for monolayer sorption on homogeneous surfaces, do not provide adequate description of the sorption data of Cs^+ and Ba^{2+} ions as suggested by the linear correlation coefficients given in Table

4.9. The correlation coefficients for Ba²⁺ data are larger than those corresponding to Cs⁺ data, however, such values for both cations are indicative of poor fits.

Table 4.9: Values of the Linear Correlation Coefficients (L.C.C) Obtained from Langmuir Fits to the Experimental Sorption Data of Cs⁺ and Ba²⁺ on Magnesite

T (K)	303	313	323	333
L.C.C of Cs ⁺	0.47	0.41	0.44	0.42
L.C.C of Ba ²⁺	0.80	0.75	0.72	0.81

4.3- Thermodynamic Parameters

Thermodynamic parameters such as the enthalpy change, ΔH° , and the entropy change, ΔS° , the Gibbs free energy change, ΔG° , and the sorption mean free energy, E , were calculated from the sorption data of Cs^+ and Ba^{2+} ions. These parameters help in viewing the sorption process thermodynamically, i.e. expressing degree of endothermicity or exothermicity, stability of sorption, type of sorption and the extent of spontaneity of the process.

Enthalpy, H , is an energy function which is adapted to processes occurring at constant pressure, the main constrain on chemical reactions. In a sorption process each species possesses a definite total enthalpy. The difference between the enthalpy summation corresponding to the sorption products and that corresponding to the sorption reactants give the enthalpy change of sorption, ΔH° . (Since no other enthalpies will be considered in this text, ΔH° together with the other thermodynamic parameters will be written without using any subscript).

An exothermic sorption process is denoted by negative ΔH° values. In such a process, low temperatures are favored, and elevated temperatures lead to decrease in the sorbed quantities. On the other hand, positive ΔH° values are used to denote endothermic processes, the case in which increasing temperatures lead to increase in sorption.

Values of enthalpy changes are related to the type of sorption and to the sorbed quantity. Typical values of ΔH° for physical sorption (sorption type(s) other than chemisorption) lie in the range of 4 - 40 kJ/mol. Such values are very small and correspond to weak sorption forces when compared to chemisorption where ΔH° values can go up to 800 kJ/mol [41].

ΔH° values were calculated from the least square fits to the experimental data using equation (2.19) which was given as:

$$\ln R_d = \frac{\Delta S^\circ}{R} - \frac{\Delta H^\circ}{RT}$$

The least square fits were obtained by plotting $\ln R_d$ versus the reciprocal of absolute sorption temperatures. These least square fits for the sorption of Cs^+ and Ba^{2+} ions on magnesite are shown in Tables 4.10 and 4.11 and plotted in Figs. 4.12 and 4.13 respectively. All ΔH° values are negative, indicating the exothermic nature of sorption for both cations. A decrease in temperature favors sorption products which are energetically stable. The decrease in sorption with the increase in temperature may be attributed to the increased desorption caused by an increase in the thermal energy of the sorbates [42]. Furthermore, the ΔH° values are within the range corresponding to physical sorption type, with those of Cs^+ sorption surpassing those of Ba^{2+} ion. No obvious concentration dependence of ΔH° values is observed for either cation.

**Table 4.10: Values of the Enthalpy Change, ΔH° , and the Entropy Change, ΔS°
Obtained from the Experimental Sorption Data of Cs^+ Ion on Magnesite**

Initial Concentration (meq/mL)	ΔH° (kJ / mol)	ΔS° (kJ / mol.K)
1.0×10^{-1}	-39	-0.106
1.0×10^{-2}	-43	-0.117
1.0×10^{-3}	-32	-0.076
1.0×10^{-4}	-54	-0.140
1.0×10^{-5}	-22	-0.034
1.0×10^{-6}	-31	-0.056
Average \pm S .D.	-37 ± 5	-0.088 ± 0.0021

**Table 4.11: Values of the Enthalpy Change, ΔH° , and the Entropy Change, ΔS°
Obtained from the Experimental Sorption Data of Ba^{2+} Ion on Magnesite**

Initial Concentration (meq/mL)	ΔH° (kJ / mol)	ΔS° (kJ / mol.K)
1.07×10^{-2}	-12	-0.014
2.15×10^{-3}	-19	-0.029
1.00×10^{-5}	-7	0.013
1.00×10^{-6}	-14	-0.005
Average \pm S .D.	-13 ± 5	-0.0088 ± 0.0017

The thermodynamic function entropy, S, may be interpreted as a measure of randomness or disorder of a system. A highly disordered system is said to have a high entropy, and every spontaneous change is accompanied by an increase in entropy. For a given substance the solid state is the state of lowest entropy (most ordered), the gaseous state is the state of highest entropy (most random), and the liquid state is intermediate between the other two.

In an sorption process, entropy changes refer to the difference between entropies of the sorbed species and entropies of these species in solution. An increase in entropy of the sorbed species gives positive ΔS° values and characterizes a more disorder or randomness of the sorbed species. Whereas a

decrease in entropy of the sorbed species yields negative ΔS° values and characterizes a more restricted motion of the sorbed ions on the adsorbent surface.

The values of the entropy change, ΔS° , obtained from the intercepts of the linear fits for sorption data utilizing equation (2.19) are shown in Tables 4.10 and 4.11. The negative signs are indicative of the stability of surface sorption for both cations. The relatively lower negative value of ΔS° suggests the presence of high energy bonds. It also indicates an ordered arrangement of the sorbate over the adsorbent [43]. Association, fixation or immobilization of the cations as a result of sorption attributed to a decrease in the degrees of freedom gives rise to negative entropy changes [36]. This implies that the motion of Cs^+ ions is more restricted than that of Ba^{2+} ions on the sorption surface and that Cs^+ species are ordered in a better way on the surface due to the existence of stronger bonding forces. In an ordered sorption, the sorption sites are filled in such a way that the sorbate forms an ordered structure on the surface at moderate coverage. One generally gets ordered sorption when there is a mixture of attractive and repulsive forces so that some sites are filled with enhanced probability while others are filled with reduced probability [44].

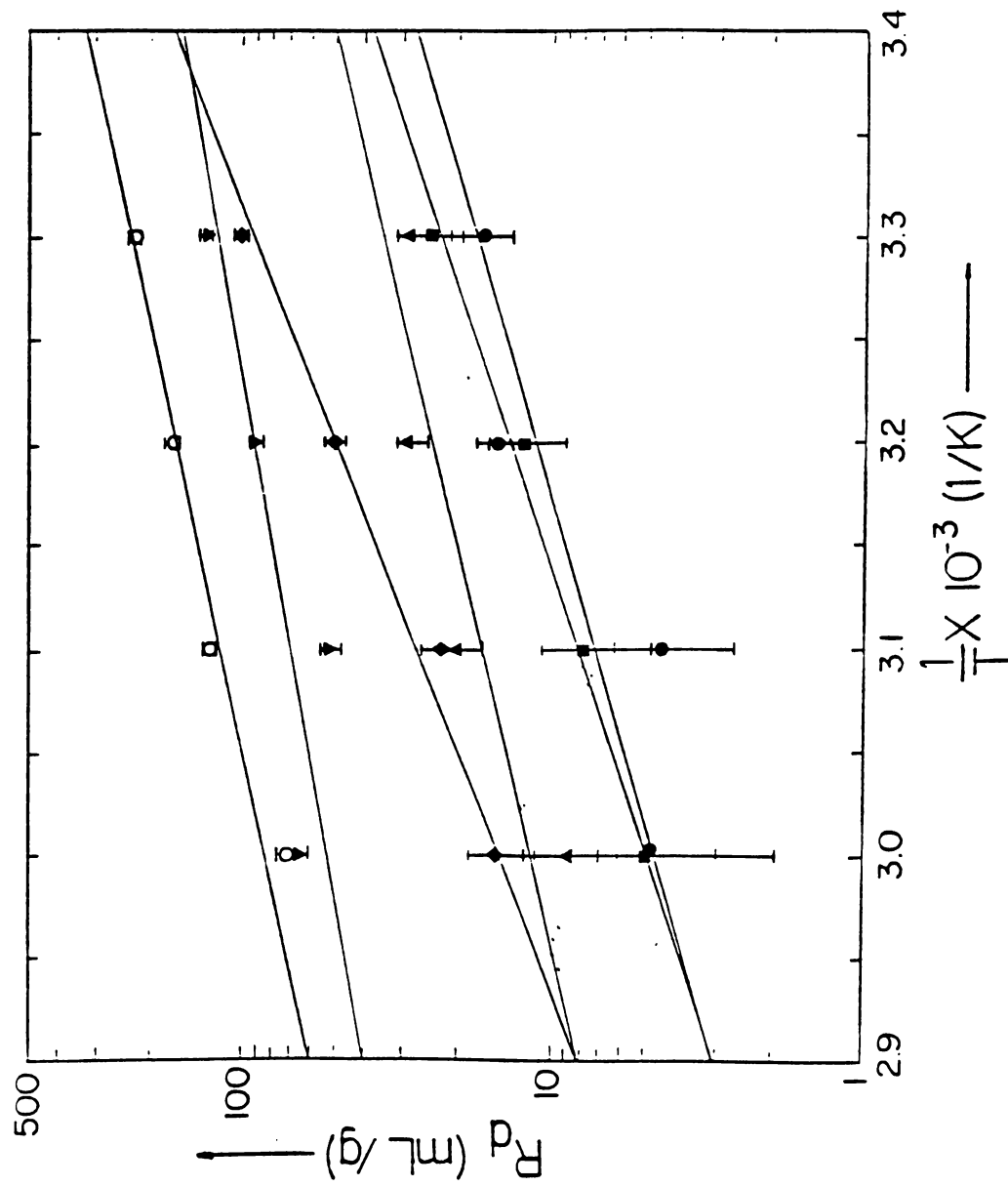


Fig. 4.12: Variation of R_d as a Function of Temperature for the Sorption of Cesium on Magnesite
 ● : 1.00×10^{-1} ■ : 1.00×10^{-2} ▲ : 1.00×10^{-3} ◆ : 1.00×10^{-4}
 ▼ : 1.00×10^{-5} ○ : 1.00×10^{-6} (meq/mL.)

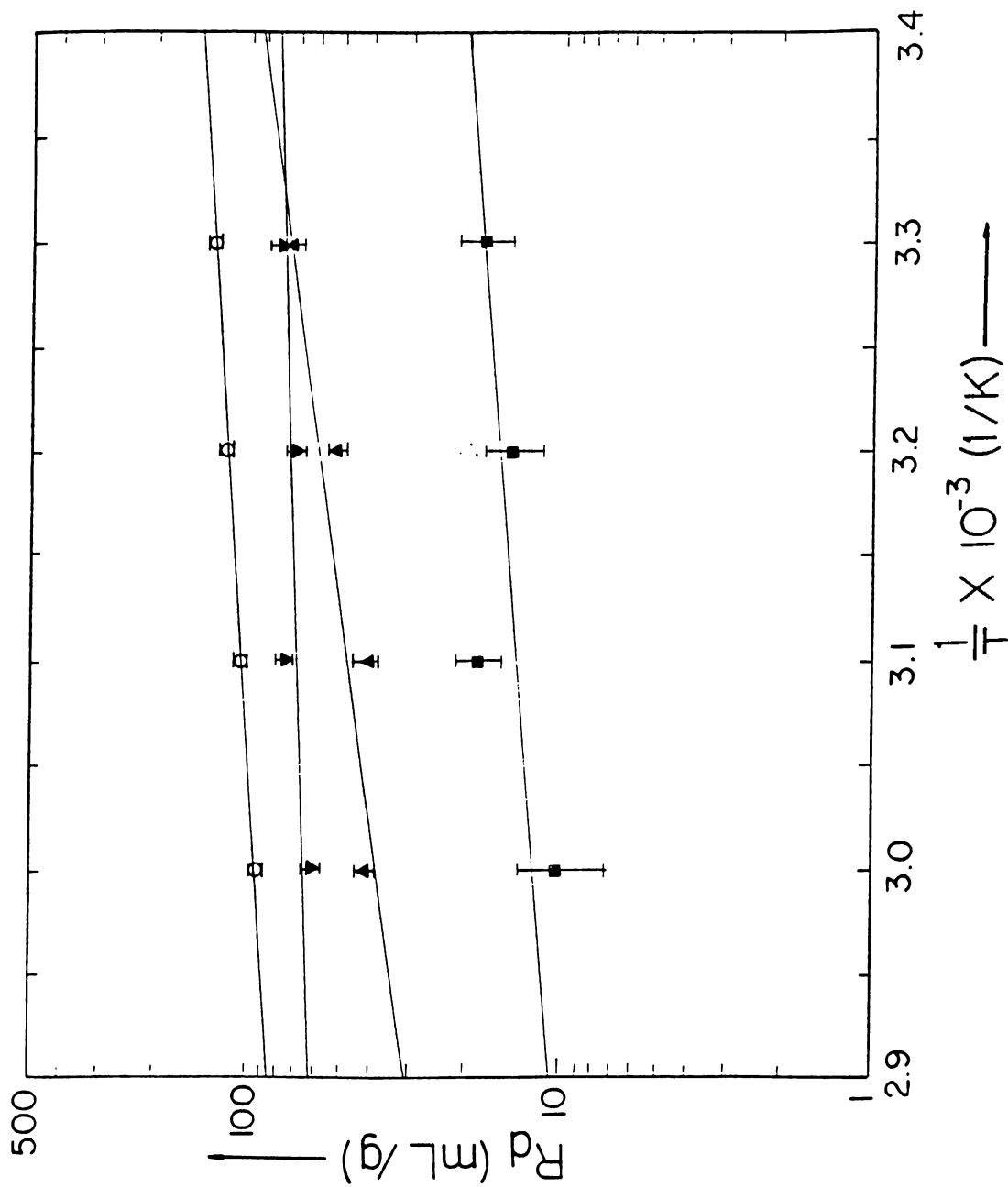


Fig. 4.13: Variation of R_d as a Function of Temperature for the Sorption of Barium on Magnesite ■ : 1.00×10^{-2} ▲ : 1.00×10^{-3} ▼ : 1.00×10^{-5} ○ : 1.00×10^{-6} (meq/ml.)

The Gibbs free energy, G , is an energy function that can be defined in terms of enthalpy and entropy ($G=H-TS$). Gibbs free energy change, ΔG° , therefore, combines two factors that influence the reaction spontaneity. A negative value of ΔH° helps to make ΔG° value negative, which indicate the spontaneity of the process. Spontaneity is also favored if ΔS° value is positive (or small in negative). The domination of one factor over the other will control the extent to which a certain process is spontaneous. A large negative value of ΔH° can, however, outweigh an unfavorable entropy change, resulting in a negative ΔG° value. Moreover, a large positive value of $T\Delta S^\circ$ can overshadow an unfavorable enthalpy change giving rise to a negative value of ΔG° . Generally, for processes occurring at low temperatures, the absolute value of ΔH° may outway that of $T\Delta S^\circ$, but for processes carried out at high temperatures the latter is generally dominant.

Gibbs free energy change of sorption, ΔG° , was calculated utilizing equation (2.17) which was expressed in the form:

$$\Delta G^\circ = - RT \ln R_d$$

This equation indicates that ΔG° is directly propotional with absolute temperature and the distribution ratio which is approximated as an equilibrium constant. Since two exchange sites exist for cesium sorption. A couple of ΔG° values were calculated at each temperature each corresponding to a different equilibrium

constant. For barium sorption, a single set of ΔG° values were calculated since a single sorption site exists.

Negative values were obtained for the sorption of both cations at all temperatures, as illustrated by Table 4.12 . Processes with negative ΔG° values, are spontaneous and energetically favored. Such processes will tend to approach minimum energy levels, and therefore, the greater the decrease in ΔG° , the more likely the process becomes favorable from a thermodynamic point of view. As can be seen from the Table 4.12, the spontaneity of Cs^+ ion sorption on both of the exchange sites decreases as temperature is increased. The numerical values of ΔG° decrease as a result of the decrease in affinity between the sorbate and the adsorbent. Another thing that can be noted is that the decrease in ΔG° values that correspond to the sorption site of high R_d values is not as drastic as it is for the exchange site of low R_d values. This shows that, as temperature is increased, Cs^+ ions tend to prefer to be sorbed on one exchange site in larger proportions relative to the second site.

Inspecting ΔG° values for Ba^{2+} ions sorptions, it can be observed that no obvious effect of temperature on the spontaneity extent of Ba^{2+} ions is observed. If the average values of ΔG° for the two sorption sites of Cs^+ ions are to be calculated, it can be seen that ΔG° values of Ba^{2+} ions sorption exceed those average values slightly, indicating that the extent of spontaneity of Ba^{2+} ions towards sorption is

some how larger and is less affected by increasing temperature as it is the case for Cs^+ ions.

Table 4.12: The Average Gibbs Free Energy Changes of Sorption, ΔG° (kJ/mol), of Cs^+ and Ba^{2+} Ions on Magnesite

Temperature (K)	Cs^+		Ba^{2+}
	First Site	Second Site	Single Site
303	-8 ± 1	-12 ± 1	-10 ± 2
313	-8 ± 1	-12 ± 1	-10 ± 2
323	-6 ± 2	-11 ± 2	-11 ± 2
333	-5 ± 2	-11 ± 2	-10 ± 2

An important fact about the magnitudes of ΔG° for the sorption of both cations is that these magnitudes lie within the 8-16 kJ/mol range which is the energy range for ion exchange type reactions [45].

The effect of temperature on the sorption of Cs^+ and Ba^{2+} ions was examined also using XPS. The experimental results showed that the amount of

Ba^{2+} ion sorbed decreases with increasing temperature, the thing that, to a certain extent, agrees with the results obtained by the radiotracer method. The experimental values of the atomic concentration ratios are given in Table 4.13 and plotted in Fig. 4.14.

Table 4.13: Values of the Atomic Concentration Ratios Obtained for Sorption Cesium and Barium on Magnesite as a Function of Temperature

Temperature (K)	Atomic Ratio(Cs/Si)	Atomic Ratio(Ba/Si)
303	0.032	0.043
313	0.028	0.047
323	0.033	0.040
333	0.033	0.037

The results obtained for Cs^+ sorption by XPS, however, show that there is no significant effect of temperature on the amount of Cs^+ sorbed. As shown in Table 4.13 and Fig. 4.14, the atomic ratios are almost constant at various temperatures. This does not agree with the experimental values obtained from the radiotracer experiments and may be attributed to the low sensitivity of XPS at small concentrations (The initial concentration used for Cs^+ and Ba^{2+} ions was 0.001 M).

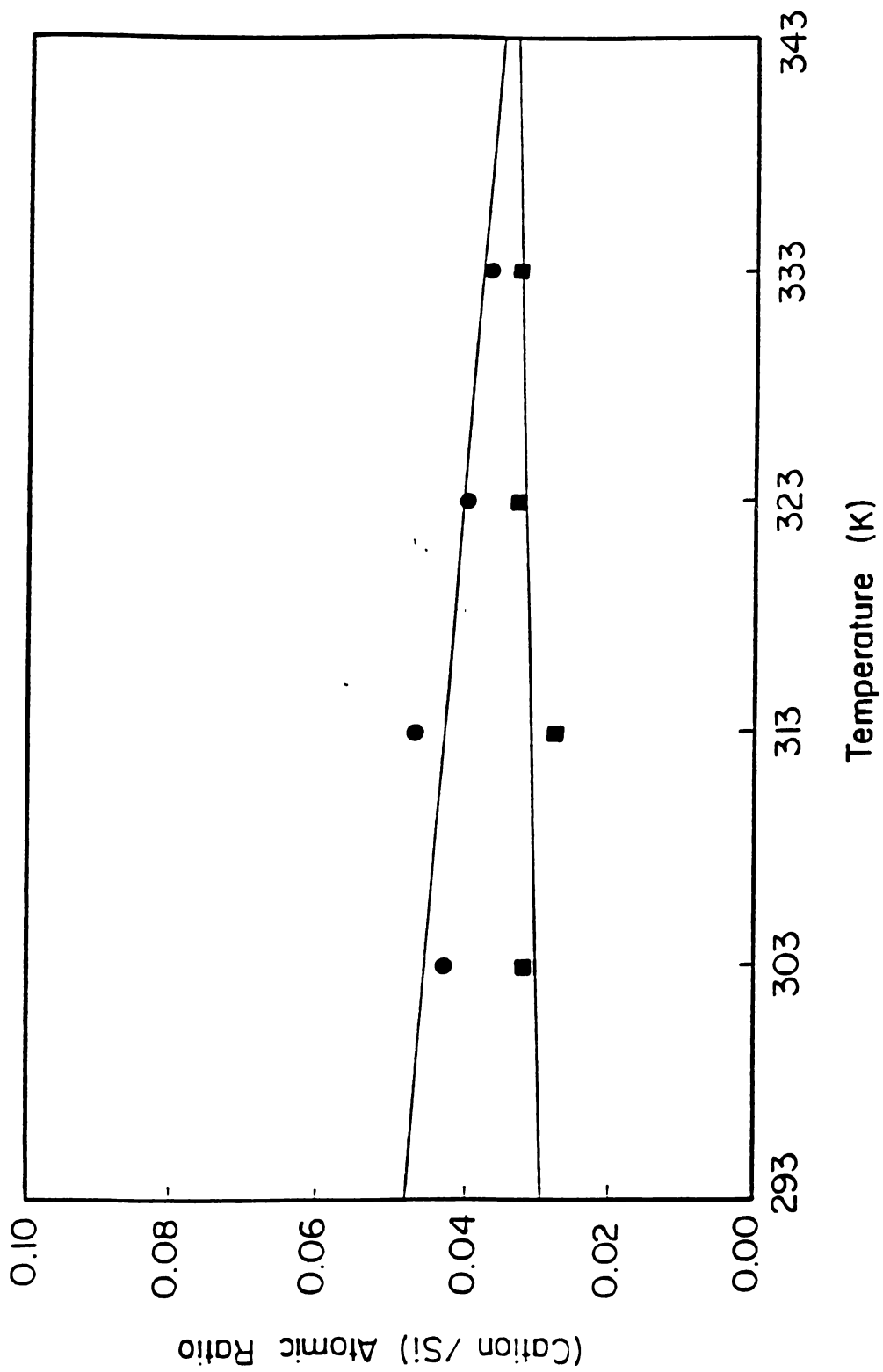


Fig. 4.14: Variation of Atomic Concentration Ratio as a Function of Temperature for Sorption of Cesium and Barium on Magnesite ■ : Cesium ion ● : Barium ion

4.4- Conclusions

Regarding the sorption of cesium and barium ions on magnesite the following conclusions can be drawn :

- According to the radiotracer and XPS studies carried out for cesium and barium sorption on magnesite, equilibrium is established within a day of contact.
- For cesium, sorption takes place primarily via two step mechanisms and/or two exchanging sites . This is indicated by the inverse S-shape loading curves. On the other hand, sorption of barium occurs via a single mechanism as suggested by the single plateau loading curve.
- The XPS studies show that the atomic concentration ratio and hence the surface coverage increases as the cation initial concentration increases for both cesium and barium ions sorption.
- Freundlich isotherms, as compared to other isotherm types provide the most adequate description of the sorption data for Cs^+ and Ba^{2+} ions at different temperatures. The values of Freundlich parameters k and n suggest that Ba^{2+} ion has a larger sorption affinity and intensity.

- The negative values and magnitudes of ΔH° and ΔS° for both ions indicate the exothermic and stable nature of sorption. The lower ΔS° value for Cs^+ suggests more ordered and stable sorption. Negative ΔG° values show that the sorption process is spontaneous. The spontaneity of Ba^{2+} ions is slightly higher than that of Cs^+ ions as indicated by these ΔG° values. The magnitudes of ΔG° for both cations at all temperatures studied suggest that ion-exchange is the main sorption mechanism.

REFERENCES

- [1] Larsson, A., Thomas, K.T. The IAEA Program for the Underground Disposal of Radioactive Wastes IAEA-CN-43/171 (1982).
- [2] Underground Disposal of Radioactive Wastes, Safety Series, No. 54, International Atomic Energy Agency, Vienna (1981).
- [3] Sorption, Modelling and Measurement for Nuclear Waste Disposal Studies. Summary of Nuclear Energy Agency Workshop held in Paris, (1983).
- [4] Tornstenfelt, B., Andresson, K., Allard, B. Sorption of Sr and Cs on Rocks and Minerals, Part 1: Sorption in Groundwater Report Prav 4.29, National Council for Radioactive Wastes, Stockholm (1981).
- [5] Vandergraaf, T.T. Review of the Role of Nuclear Analytical Chemistry in the Canadian Nuclear Fuel Waste Management Program. J. Radioanal. Nucl. Chem., 110, 79-89 (1987).
- [6] Krezova, V.J. Radionuclides Migration in the Geosphere and Their Sorption on Natural Sorbents. J. Radioanal. Nucl. Chem., 208/2, 559-575 (1996).

- [7] Final Storage of Spent Nuclear Fuel -KBS-3, III Barriers Swedish Nuclear Fuel Supply Co / Division KBS, Stockholm, Sweden (1983).
- [8] Gillman, G.P. A Proposed Method for the Measurement of Exchange Properties of Highly Weathered Soils. *Aust. J. Soil Res.*, 17, 129-139 (1979).
- [9] Tucher, B.M. A Proposed New Reagent for the Measurement of Cation Exchange Properties of Carbonate Soils. *Aust. J. Soil Res.*, 23, 633-642 (1985).
- [10] Matsue, N., Wada, K. A New Equilibrium Method for Cation Exchange Capacity Measurement. *Soil Sci. Soc. Am. J.*, 49 (1985).
- [11] Searle, P.L. The Measurement of Soil Cation Exchange Properties Using the Single Extraction, Silver Thiourea Method. *Aust. J. Soil Res.*, 24, 193-200 (1986).
- [12] Harrison, R.M., de More, S.J., Repsomanikis, S., Johnston, W.R. *Introductory Chemistry for the Environmental Sciences*. Cambridge University Press (1991).
- [13] Sundstrom, D.W., Klei, H.E. *Waste Water Treatment*. Prentice-Hall Inc.
- [14] Berry, J.A., Bourke, P.J., Coates, H.A., Green, A., Jafferries, N.N., Littleboy, A.K. Sorption of Radionuclides on Sandstones and Mudstones. Presented in International Conference on Chemistry and Migration Behavior of Actinides and Fission Products in the Geosphere, Munich (1987).
- [15] Aksoyoglu, S. Ph.D Thesis, Middle East Technical University (1987).
- [16] Hatipoglu, S. M.Sc. Thesis, Middle East Technical University (1987).

- [17] Erten, H.N. , Aksoyoglu, S., Gokturk, H. Sorption/Desorption of Cs on Clay and Soil Fractions from Various Regions of Turkey. *Sci. Total Environ.*, 69, 269-296 (1988).
- [18] Eylem, C. M.Sc. Thesis. Middle East Technical University (1988).
- [19] Gokmenoglu, Z. M.Sc. Thesis. Bilkent University (1991).
- [20] Wilson, M.J. *Clay Mineralogy: Spectroscopic and Chemical Determinative Methods*. Chapman & Hall (1994).
- [21] Bancroft, G.M., Brown, J.R., Fyfe, W.S. Quantitative X-Ray Photoelectron Spectroscopy (ESCA) : Studies of Ba sorption on Calcite. *Chem. Geol.*, 19, 131-144 (1977).
- [22] Briggs, D., Seah, M. *Practical Surface Analysis, Volume 1, Auger and X-ray Photoelectron Spectroscopy*, Wiley (1990).
- [23] Brouwer, E., Baeyers, B., Cramers, A. Cesium and Rubidium Ion Equilibria in Illite Clay. *J. Phys. Chem.*, 87, 1213-1219 (1986).
- [24] Brule, D.G., Brown, J.R., Bancroft, G.M., Fyfe, W.S. Cation Sorption by Hydrous Manganese Dioxide, A Semi Qualitative X-Ray Photoelectron Spectroscopy (ESCA) Study. *Chem. Geol.*, 28, 331-339 (1980).
- [25] Davison, N., Mc Whinnie, W.R., Hoper, A. X-Ray Photoelectronic Spectroscopic Study of Cobalt (II) and Nickel (II) Sorbed on Bacterite Montmorillonite. *Clays and Clay Minerals*, 39, 22-27 (1991).

- [26] Dillard, J.G., Koppelman, M.H. X-Ray Photoelectron Spectroscopic (XPS) Surface Characterization of Cobalt on the Surface of Kaolinite. *J. Colloid Interface Sci.*, 87, 46-55 (1982)
- [27] Koppelman, M.H., Emerson, A.B., Dillard, J.G. Sorbed Chromium (III) on Chlorite, Illite and Kaolinite: An X-Ray Photoelectron Spectroscopic Study. *Clays and Clay Minerals*, 28, 119-124 (1980).
- [28] Perry, D.L. Application of Surface Techniques to Chemical Bonding Studies of Minerals. *Am. Chem. Soc.*, 389-402 (1986).
- [29] Cornelis, K., Cornelius, S., Hulburt, Jr. *Manual of Mineralogy*, John Wiley and Sons Inc. (1985).
- [30] Dear, W.A., Howie, R.A., Zussman, J. *An Introduction to the Rock Forming Minerals*, Longman and Scientific Technical (1985).
- [31] Bates, L.R. *Geology of the Industrial Rocks and Minerals*, Dover Publication Inc. (1969).
- [32] Worrall, W.E. *Clays and Ceramic Raw Materials*, Elsevier Applied Science Publication (1986).
- [33] Stumm, W. *Chemistry at the Solid-Water Interface*. John Wiley and Sons Inc. (1992).
- [34] Chastain, J. *Handbook of X-Ray Photoelectron Spectroscopy*. Perkin-Elmer Co. (1992).
- [35] Scofield, JH. Hartree-Slater Subshell Photoionization Cross Sections at 1254 and 1487 eV. *J. Elect. Spect.*, 8, 129-137 (1976).

- [36] Khan, S.A., Reman, R., Khan, M.A. Sorption of Cs(I), Sr(II) and Co(II) on Al_2O_3 . *J. Radioanal. Nucl. Chem.*, 190, 81-96 (1995).
- [37] Qadeer, R., Hanif, J., Saleem, M., Afzal, M. Surface Characterization and Thermodynamics of Sorption of Sr^{2+} , Ce^{3+} , Sm^{3+} , Gd^{3+} , Th^{4+} and Uo^{2+} on Activated Charcoal from Aqueous Solution. *Colloid Polym. Sci.*, 271, 83-90 (1993).
- [38] Kumari, K., Singh, R.P. Sorption Thermodynamics of Cypermethrin at High Concentrations on Some Indian Soils. *Intern. J. Environ. Anal. Chem.*, 53, 115- 124 (1993).
- [39] Mishra, S. P., Tiwary, D. Ion Exchangers in Radioactive Waste Management. *J. Radioanal. Nucl. Chem.*, 196/2, 353-361 (1995).
- [40] Kozai, N., Ohunki, T., Matsumoto, J., Banba, T., Ito, Y. A Study of Specific Sorption of Neptunium (V) on Smectite in Low pH Solutions. *Radiochemica Acta*, 75, 149-158 (1996).
- [41] Levine, I. N. *Physical Chemistry*. McGraw Hill (1988).
- [42] Panday, K. K., Prasad, J., Singh, V. N. Removal of Cr(VI) from Aqueous Solutions by Adsorption on Fly Ash-Wollastonite. *J. Chem. Tech. Biotech.*, 34A, 367-374 (1984).
- [43] Sundaram, K. M. S. Adsorption Behavior of RH-5992 Insecticide Onto Sandy and Clay Loam Forest Soils. *J. Environ. Sci. Health.*, B 29(3), 415-442 (1994).

[44] Masel, R. I. Principles of Adsorption and Reaction on Solid Surfaces. John Wiley and Sons Inc. (1996).

[45] Helfferich, F. Ion Exchange. McGraw Hill (1962).